forests

MDPI

Article

Priority Effect of Endophyte Community in Newly Fallen Leaves of *Quercus acutissima* Carruth. on Litter Decomposition and Saprotrophic Microbial Community

Dongmei Yang [1], Yonghui Lin [1], Zaihua He [1], Xingbing He [1,*] and Xiangshi Kong [2]

[1] College of Biology and Environmental Sciences, Jishou University, Jishou 416000, China
[2] College of Tourism and Management Engineering, Jishou University, Zhangjiajie 427000, China; kongxiangshi@126.com
* Correspondence: hexb@jsu.edu.cn

Abstract: This study examines the role of endophytic microbial colonization on the decomposition of oak leaf litter, a high-quality substrate in forest ecosystems. Over a one-year incubation, we observed a significant reduction in mass loss in colonized litter (46%) compared to non-colonized litter (80%), indicating an inhibitory effect of endophytes on decomposition. Structural equation modeling revealed a bimodal impact of endophytic microbes, with an initial enhancement followed by a pronounced inhibition as decomposition progressed. Extracellular enzyme stoichiometry showed phosphorus limitation became significant, particularly with endophytic colonization, contributing to reduced decomposition rates. Microbial diversity analyses exposed the variable impacts of endophytic colonization on fungal and bacterial communities, with taxa such as Helotiales (order) and *Burkholderia–Caballeronia–Paraburkholderia* (genus) significantly affected. The identification of 16 keystone species, mostly endophytic bacteria, underscored their pivotal influence on decomposition processes. Despite initial endophytic impacts, abundant carbon resources promoted stochastic colonization, potentially surpassing the effects of early endophytic establishment. This study provides insights into the priority effects of endophytic colonization and niche differentiation, offering a foundation for further research into the mechanisms underlying these processes and their ecological consequences in various ecosystems.

Keywords: microbial community assembly; microbial co-occurrence network; extracellular enzyme stoichiometry; microbial diversity; microbial source tracking

Academic Editors: Jiwei Li and Kaibo Wang

Received: 31 December 2024
Revised: 24 January 2025
Accepted: 26 January 2025
Published: 28 January 2025

Citation: Yang, D.; Lin, Y.; He, Z.; He, X.; Kong, X. Priority Effect of Endophyte Community in Newly Fallen Leaves of *Quercus acutissima* Carruth. on Litter Decomposition and Saprotrophic Microbial Community. *Forests* **2025**, *16*, 249. https://doi.org/10.3390/f16020249

1. Introduction

Litter decomposition is a pivotal process in forest ecosystems, essential for nutrient cycling and carbon sequestration. It is influenced by a multitude of abiotic and biotic factors; climatic conditions play a predominant role at the regional scale [1], while litter quality and decomposer communities are crucial at the local scale [2]. Microbial communities are central to this process, with endophytes modulating litter decomposition rates in terrestrial systems [3]. Endophytes, a hyperdiverse group encompassing bacteria and fungi, colonize a broad range of host plants and tissues across ecosystems from tropical to boreal [4]. Their ecological role extends beyond the symbiotic phase to the litter decomposition phase [5].

The literature presents a dichotomy, with some studies reporting increased decomposition rates due to endophyte presence [6–11], while others observe a decrease [3,12–15]. This variability suggests that the role of endophytes in decomposition is context-dependent

and may be influenced by factors such as endophyte species, host plant species, and environmental conditions.

Understanding the controls of litter decomposition is vital for estimating carbon budgets in ecosystems [16]. Plant endophytes may affect decomposition through various pathways: they can compete for organic substrates with later-arriving saprotrophic invaders and alter litter quality by modifying components, such as endophytic alkaloids and elemental contents [15,17]. These changes can directly affect decomposition rates or indirectly influence microbial decomposers and the decomposition microenvironment, potentially altering litter degradation [18]. Many endophytes have the capability to decompose leaf litter by producing cellulolytic and/or ligninolytic enzymes [6,7,10,13]. A considerable proportion of leaf endophytes can persist into 1-year-old litter [19,20]. Furthermore, some grass endophytes, such as *Epichloë* spp., are obligate symbionts that cannot survive in senesced plant litter but can produce alkaloids that alter litter chemistry, potentially cascading through decomposition processes [14,21]. The presence of endophytes, particularly those producing secondary compounds, like alkaloids and phenolics, is hypothesized to inhibit decomposer microbe activity, thereby slowing decomposition [22]. However, for endophytes within tree leaves, there is no evidence to suggest that these endophytes produce secondary metabolites that would affect subsequent decomposition. Instead, growing evidence suggests that some endophytes become saprobes after leaf fall [23–25]. Their endophytic occurrence might thus be just one stage in their life cycle, persisting in litter to complete their life cycle [26]. As pioneer colonizers, they can take advantage of accessible chemical compounds and possess the enzymatic machinery to degrade complex structural plant compounds, such as cellulose and lignin [27,28]. The ability of endophytes to persist in litter and compete with other decomposers suggests that they may act as keystone species, significantly influencing the structure and function of decomposer communities [19].

The majority of research examining the role of endophytes in decomposition has centered on individual species, predominantly within the context of herbaceous plants [21,29]. These plants' endophytes often exist in a dominant single-species form in their natural state, facilitating the study of endophyte impact on litter decomposition. By contrast, endophytes within tree leaves often exhibit a co-dominance of multiple species, and their entry into litter introduces a complexity of traits that makes their interactions and impact on the decomposition process extremely intricate. Consequently, few studies have examined the colonization of endophytic communities during the decomposition process and their subsequent impact. Many endophytic species from tree leaves have the capacity to utilize litter [30], and these fungi interact with subsequent colonizers, affecting the degradation process. Endophytes influence microbial community composition and the decomposition process through a priority effect [7,19,22,31,32]. While the members of the endophytic community may not uniformly affect litter decomposition due to trait differences, the community of endophytes from the same host plant represents an adaptive evolutionary response to the plant, with members forming close positive associations. Additionally, the priority colonization of endophytes is a significant event in the historical assembly of microbial communities [4,7], and any event in this assembly history can influence subsequent ecological processes, including decomposition processes and microbial community assembly [33,34]. Therefore, we hypothesize that the priority effect of endophytes at the initial stages of decomposition will shape the succession of microbial communities and their enzymatic profiles, thereby influencing the overall decomposition process. Beyond the priority effect, the persistent ability of endophytes in the litter decomposition process is also a crucial manifestation of their impact on the composition of saprotrophic communities and their decomposition functions [19,20]. After endophytes enter the saprotrophic system, a significant portion

of them, as saprophytes, can participate in litter decomposition, with keystone species potentially persisting until the end of the decomposition process. Therefore, we propose the second hypothesis that endophytic communities will continue to influence microbial composition and decomposition functions after entering the decomposition process of oak leaf litters, with keystone endophytes exerting a significant impact.

This study investigates the priority effect of naturally occurring endophytic communities in newly fallen leaves of *Quercus acutissima* Carruth. on litter decomposition and the subsequent impact on saprotrophic microbial communities. Our aim is to elucidate the role of endophytes in shaping the decomposition process and their interaction with saprotrophic microbes, providing insights into the complex dynamics of microbial communities in forest ecosystems.

2. Materials and Methods

2.1. Experimental Site and Litter Collection

The experimental site is located in the oak (*Q. acutissima*) forest of Zhailong Village (25°52′–31°24′ N and 107°4′–112°2′ E), Jishou City, in the Wuling Mountain region of China. This region is characterized by a subtropical monsoon climate, with an average annual temperature ranging from 12 °C to 17 °C and an annual precipitation of 1100 to 1600 mm. The landscape is dominated by mountainous and hilly terrain with steep slopes and complex geographical features. This unique environment supports rich biodiversity, with various types of subtropical forests, including broad-leaved and coniferous forests. In this study, we selected the leaf litter of oak, a widely distributed species in this region. The oak trees in our study site are approximately 50 years old, with a height ranging from 10 to 15 m, and an average leaf size of 4 cm × 16 cm. Oak leaf litter plays a significant role as one of the primary sources of soil nutrient input and greatly contributes to the regional carbon cycle.

2.2. Field Experiment Design for Litter Decomposition

Leaf litter samples were meticulously collected at the apex of the leaf-fall season in November. To ensure the leaves remained uncontaminated by soil, we employed a method of gently agitating the oak trees to dislodge the newly fallen leaves, which were then carefully intercepted using suspended nylon nets at the height of 1.5 m. The collected leaves were placed into sterile, resealable plastic bags. These sample bags were covered with ice and then promptly transported to the laboratory and stored at −4 °C to preserve their freshness prior to analysis. A total of 135 freshly collected leaf samples, each weighing approximately 15.0 g, were subjected to meticulous preparation for subsequent analysis. To ascertain the initial dry weight of the leaf litter, five representative samples were selected and oven-dried at a temperature of 50 °C until they reached a constant weight. This process yielded a conversion factor, with the fresh weight equivalent to approximately 6.2 g on a dry weight basis. The remaining 130 samples were subjected to three treatments, as follows: 1. Natural state (NS, 45 samples): This group served as control, with no interventions applied to the leaves; 2. Surface sterilization (SS, 45 samples): In this treatment, the efforts were made to eliminate epiphytic microbes from the leaf surfaces; 3. Irradiation sterilization (IS, 40 samples): This treatment was designed to eliminate all microorganisms residing within the leaf tissues. In the natural state (NS) and surface sterilization (SS) treatments, 5 samples each were placed in sterilized tubes and stored at −80 °C for the assessment of the initial microbial composition of the freshly fallen leaves prior to the experiment about litter decomposition. Next, 120 samples were evenly distributed across above three treatments for litter decomposition. The treated leaf litter samples were then placed into sterile nylon mesh bags measuring 20 cm × 20 cm with a mesh size of 1 mm. The samples designated

for surface sterilization (SS) treatment were processed in accordance with the methodology detailed by He et al. [30]. The samples for irradiation sterilization (IS) treatment were dispatched to BIOZERN Biotech. Co., Ltd. for sterilization with gamma rays at a dosage of >22 kGy. In December 2022, the prepared litter bags were placed in the organic layer of the soil in three randomly selected plots of the oak forest (each plot measuring 2 m × 2 m and spaced 5 m apart). Sampling was conducted at four time points: 6 January 2023 (T1), 6 March 2023 (T2), 6 June 2023 (T3), and 6 December 2023 (T4). At each time point, 10 litter bags were randomly collected (5 samples for analyzing microbial extracellular enzyme activity, carbon dioxide release and microbial community, and 5 samples for assessing mass loss). The collected samples were placed in sterile ziplock bags on ice and returned to the laboratory for processing.

2.3. Extracellular Enzyme Activity, Carbon Dioxide Release, and Remaining Mass

After brushing off the soil adhering to the litter, the leaves were cut into small pieces and homogenized into a slurry using a mortar and pestle with a buffer solution. The homogenate was centrifuged, and the supernatant was collected for enzyme activity measurement. The enzyme activities of β-glucosidase (E.C. 3.2.1.21, βG), exocellulase (E.C. 3.2.1.91, C1), and endocellulase (E.C. 3.2.1.4, Cx) were measured using the DNS (3,5-dinitrosalicylic acid, MACKLIN, Shanghai, China) method as described by Agnihotri et al. [35]. The activities of β-N-acetylglucosaminidase (E.C. 3.2.1.30, NAG) and acid phosphatase (E.C. 3.1.3.2, AP) were measured using the p-nitrophenol (pNP) method, as described by Sinsabaugh et al. [36]. In this method, pNP derivatives are used as substrates, which release measurable pNP upon hydrolysis. The substrates for NAG and AP were pNPN-acetyl-4-D-glucosaminide (MACKLIN, Shanghai, China) and p-nitrophenyl (pNP, MACKLIN, Shanghai, China) phosphate, respectively. The detailed measurement procedures can be found in Li et al. [37]. Leucine aminopeptidase (E.C. 3.4.11.1, LAP) activity was measured using the p-nitroaniline (pNA) method [38], with L-leucine-p-nitroanilide (Leu-pNA, MACKLIN, Shanghai, China) as the substrate. Enzyme activities were calculated into the unit of substrate hydrolysis product per gram per hour (μM g^{-1} h^{-1}).

Approximately 0.5 g of leaf litter was placed in a sealed flask and incubated in the dark at 25 °C for 2 days. The released CO_2 was absorbed using a 0.5 M NaOH (MACKLIN, Shanghai, China) solution and measured by a two-phase titration method with 0.05 M HCl (MACKLIN, Shanghai, China) [39]. The CO_2 release from litter was expressed as μmol g^{-1} dry litter d^{-1}.

On each sampling date, five litter bags were sampled from each treatment for analysis of mass change. Gently remove soil particles from the litter leaves using a small brush. The leaves were oven-dried at 50 °C until a constant weight was achieved. Then, on each sampling date, the mass loss of the litter leaves in each litter bag was measured as the difference in weight before in situ exposure (time 0) and after exposure (time X). The data are expressed as the percentage of remaining mass relative to the initial dry mass.

2.4. DNA Extraction, PCR Amplification, and NovaSeq Sequencing

Samples in their natural state and those subjected to surface sterilization for newly fallen leaves, along with decomposed litter samples at each sampling interval, were meticulously collected for subsequent microbial sequencing analysis. Total DNA of samples was extracted according to the instructions of the E.Z.N.A.® Soil DNA Kit (Omega Bio-Tek, Norcross, GA, USA). The concentration of the extracted DNA was measured using a NanoDrop 2000 spectrophotometer (Thermo Fisher Scientific, Waltham, MA, USA). Additionally, the integrity of the DNA was assessed using 1% agarose gel electrophoresis (model: bio-west agarose, Biowest, Madrid, Spain). PCR amplification of the DNA was

conducted using a GeneAmp® 9700 PCR System (ABI, Dublin, CA, USA). The fungal community composition was determined by amplifying the ITS1 region using primer ITS1F (5′-CTTGGTCATTTAGAGGAAGTAA-3′) and ITS2R (5′GCTGCGTTCTTCATCGATGC-3′). The 16 S V5–V7 region was amplified with primers 799 F (5′-AACMGGATTAGATACCCKG-3′) and 1193 R (5′- ACGTCATCCCCACCTTCC-3′). The detailed processes of PCR and library construction are found in Zhao et al. [40]. Finally, the libraries were sequenced using an Illumina NovaSeq PE250 platform (model: NovaSeq 6000, Illumina, San Diego, CA, USA) at BIOZERN Biotech. Co., Ltd. (Shanghai, China).

The raw sequencing reads were quality-checked using Trimmomatic V0.39 to remove low-quality sequences. The effective sequences of all samples were assembled using FLASH software (Version 1.2.7). Operational taxonomic units (OTUs) were clustered with 97% similarity cutoff using UPARSE (Version 10, http://drive5.com/uparse/ (accessed on 5 April 2024)) and chimeric sequences were identified and removed using UCHIME. The phylogenetic affiliations of each ITS and 16S rRNA gene sequence were assigned using the UCLUST algorithm and compared against the UNITE (Version 8.2) database (http://unite.ut.ee/index.php (accessed on 5 April 2024)) and the SILVA (SSU138.1) database (http://www.arb-silva.de (accessed on 6 April 2024)) with a confidence threshold of 80%. The raw reads have been deposited in the NCBI Sequence Read Archive under accession number PRJNA1201886.

2.5. Leaf Litter Extracellular Enzyme Stoichiometry (EES)

To understand how exoenzyme activity reflects the microbial acquisition of carbon (C), nitrogen (N), and phosphorus (P) resources, we analyzed the stoichiometric ratios of C, N, and P based on the relative activities of key exoenzymes (such as β-glucosidase (βG), acid phosphatase (AP), N-acetyl-β-glucosaminidase (NAG), and leucine aminopeptidase (LAP)) using quantitative vector analysis [41,42]. The vector length (dimensionless) quantifies the relative limitations of carbon (C), nitrogen (N), and phosphorus (P) on microbial activity. A larger vector length value indicates a stronger relative limitation of carbon (C) on microbial activity. The angle between vectors (°) quantifies the relative limitation of phosphorus (P) and nitrogen (N) on microbial activity [42–44]. An angle between vectors greater than 45° indicates that microbial metabolism is limited by phosphorus (P), while an angle less than 45° signifies that microbial metabolism is constrained by nitrogen (N) [45]. The calculations for vector length and angle are as follows:

$$\text{Vector length} = \sqrt[2]{\left[\frac{Ln(BG)}{Ln(NAG+LAP)}\right]^2 + \left[\frac{Ln(BG)}{Ln(AP)}\right]^2}$$

$$\text{Vector angle} = \text{Degrees}\left\{ATAN2\left[\frac{Ln(BG)}{Ln(AP)}\right], \left[\frac{Ln(BG)}{Ln(NAG+LAP)}\right]\right\}$$

In the equation, ATAN2 represents the angle of the arc tangent from the origin to the point (Ln BG/Ln AP, Ln BG/Ln (NAG + LAP)), and "Degrees" indicates the tangent angle.

The ratios of C/P and C/N acquisition enzymes can reveal differences in relative resource allocation for the acquisition of C, N, and P [41]. It can also indicate the overall relative enzyme activity ratios of C/N [42]. The ratios of enzyme C, N, and P ($E_{C:N}$, $E_{C:P}$, and $E_{N:P}$) are calculated using the following formulas:

$$E_{C:N} = \frac{Ln(BG)}{Ln(NAG+LAP)}$$

$$E_{C:P} = \frac{Ln(BG)}{Ln(AP)}$$

$$E_{C:N} = \frac{Ln(NAG+LAP)}{Ln(AP)}$$

2.6. Leaf Litter Organic Matter Quality

The relative decomposition degree and recalcitrance of leaf litter organic matter are represented by the ratios of Fourier transform infrared (FTIR, Shimadzu, Kyoto, Japan) spectral bands [46]. Samples were mixed with potassium bromide (KBr, MACKLIN, Shanghai, China) at a ratio of 1:100 and analyzed using a Fourier transform infrared spectrometer (Spectrum Two, Perkin Elmer, Waltham, MA, USA). All samples were scanned at a resolution of 4 cm^{-1} for 32 scans, covering a spectral range of 4000–400 cm^{-1}, with KBr used as the background [47]. The infrared absorption bands are represented by the following functional groups: polysaccharide C-O, aliphatic C-H, aromatic C=C, and aromatic C-H. Index I is represented by the ratio of aromatic to aliphatic functional groups; a higher ratio indicates a greater degree of organic matter decomposition [43,46]. Index II represents the relative relationship between carbon (aromatic and aliphatic compounds) and oxygen-containing functional groups (polysaccharides). An increase in this value indicates greater resistance to decomposition and a reduction in biological activity [43]. The calculations for Index I and Index II are as follows:

$$\text{IndexI} = \frac{RAISB_{aromatic\ C=C+aromatic\ C-H}}{RAISB_{aliphatic\ C-H}}$$

$$\text{IndexII} = \frac{RAISB_{aliphatic\ C-H+aromatic\ C=C+aromatic\ C-H}}{RAISB_{polysaccharide\ C-O}}$$

In the equation, the denominator of Index I represents the relative area of the infrared absorption band (RAISB) of aliphatic functional groups (aliphatic C-H), while the numerator represents RAISB of aromatic functional groups. In Index II, the denominator represents RAISB of oxygen-containing functional groups (polysaccharide C-O), while the numerator represents RAISB of carbon functional groups (aromatic C=C, aromatic C-H and aliphatic C-H).

2.7. Statistical Analysis

An ANOVA analysis followed by Duncan's multiple comparisons was employed to compare the significant differences among treatments in enzyme activity, carbon dioxide release, remaining mass, organic matter quality, enzyme vector angles, enzyme vector lengths, and EES. A Kruskal–Wallis test was used to analyze the differences in microbial alpha diversity among treatments. Subsequent post hoc analysis was conducted using Dunn's test to identify specific differences between treatment groups. A significance level of $p < 0.05$ was considered statistically significant for all analyses. All analyses were conducted using R version 4.3.3.

2.7.1. Microbial Diversity

We calculated the alpha diversity indices (including Chao1, PD, Shannon, and Simpson) of bacteria and fungi using OTU richness data and phylogenetic data. Also, we calculated the alpha diversity indices of endophytic microbe at each decomposition stage to comprehensively assess their changes. These analyses were conducted using the vegan (for Shannon, Simpson, and Chao1) and picante (for PD) packages in R software version 4.3.3. Microbial beta diversity was assessed using principal coordinate analysis (PCoA), based on standardized OTU data to calculate Bray–Curtis distances using the vegan package in R [48]. To assess the differences in microbial community composition, we conducted a multivariate analysis of variance (PERMANOVA) based on Bray–Curtis distances using the adonis2 function. Additionally, to explore the relationship between microbial community composition and litter decomposition, we evaluated the correlations between bacterial and fungal alpha diversity and various indicators of the decomposition process under different treatments using Spearman correlation analysis.

2.7.2. Microbial Community Assembly

To quantify the contributions of the priority effect of leaf endophytic microbe to the microbial community assembly during leaf litter decomposition. We employed the null model statistical framework developed by Stegen et al. [49]. We calculated the Raup–Crick index (RCI) and the beta Nearest Taxon index (βNTI) using the NST package in R (https://github.com/DaliangNing/NST (accessed on 10 August 2024)), based on phylogenetic and abundance data to identify deterministic and stochastic processes of community assembly [50]. By comparing the βNTI and RCI values across different treatments and decomposition stages, we can identify the contributions of heterogeneous selection, homogeneous selection, dispersal processes, and drift in community assembly. βNTI is a null model test based on phylogenetic βMNTD (beta mean nearest taxon distance), used to characterize the turnover in phylogenetic community composition [51]. $|\beta NTI| > 2$ indicates that the turnover between observed pairs of communities is primarily driven by deterministic processes, which can be categorized into homogeneous selection ($\beta NTI < -2$) and heterogeneous selection ($\beta NTI > +2$) [52]. $|\beta NTI| < 2$ and $|RCI| > 0.95$ indicate the presence of dispersal processes, which can be further classified into homogenizing dispersal ($RCI < -0.95$) and dispersal limitation ($RCI > +0.95$). If $|\beta NTI| < 2$ and $|RCI| < 0.95$, then drift (referred to as "undominated" process) drives the compositional turnover process [49].

2.7.3. Co-Occurrence Network Analysis

To assess the complex interactions among microorganisms and identify potential keystone for each treatment during the decomposition period, we conducted a network analysis. To avoid spurious correlations, we filtered out fungal and bacterial OTUs with relative abundances less than 0.01% and those occurring in fewer than 80% of the samples. We employed the Hmisc package in R to calculate the Spearman rank correlations among all OTUs for each treatment. We applied false discovery rate (FDR) correction to adjust for multiple comparisons in the Spearman rank correlations. We removed correlations with Spearman's coefficient less than 0.8 and *p*-values greater than 0.01, which facilitated the identification of strongly correlated operational taxonomic units (OTU) [53]. We constructed an undirected network using the igraph R package and obtained the network topology parameters. We utilized the interactive platform Gephi (https://gephi.org/ (accessed on 20 August 2024)) to visualize the network using the Fruchterman–Reingold layout [54]. Subsequently, we calculated the within-module connectivity (Zi) and between-module connectivity (Pi) using the igraph package in R. Based on these two metrics, we classified the nodes in the network into four categories: peripheral nodes ($Zi < 2.5$ and $Pi < 0.62$), connector nodes ($Zi < 2.5$ and $Pi > 0.62$), module hubs ($Zi > 2.5$ and $Pi < 0.62$), and network hubs ($Zi > 2.5$ and $Pi > 0.62$). Among these, connector nodes ($Zi < 2.5$ and $Pi > 0.62$), module hubs ($Zi > 2.5$ and $Pi < 0.62$), and network hubs ($Zi > 2.5$ and $Pi > 0.62$) were considered to be keystone OTU. For more detailed methods and information, refer to Guimerà and Amaral [55] and Tang et al. [56]. To explore the relationship between the identified keystone species and the ecological functions of microorganisms involved in litter decomposition, we performed a Spearman correlation analysis between the abundance data of the identified keystone taxa and enzyme activity, extracellular enzyme stoichiometry, and organic matter quality.

2.7.4. LEfSe Analysis

We employed the LEfSe (linear discriminant analysis effect size) method, as proposed by Segata et al. [57], to identify microbial taxa with significant differences between treatment groups. LEfSe first detects significant differences in species abundance between groups using the Kruskal–Wallis rank-sum test, followed by the Wilcoxon rank-sum test to ensure

a consistency of differences between groups. Finally, linear discriminant analysis (LDA) is applied to calculate the effect size of each biomarker, quantifying its contribution to group differences [58]. We applied an LDA threshold of 3.0 and a significant p-value ($p < 0.05$) to detect biomarkers [59]. The LEfSe analysis was conducted in R using the microeco package (https://chiliubio.github.io/microeco_tutorial/model-based-class.html#trans_diff-class (accessed on 5 September 2024)).

2.7.5. Source Tracking Analysis

To investigate the changes in endophytic fungi at various decomposition stages, we employed the FEAST source tracking method proposed by Shenhav et al. [60], with R script developed by Li et al. [61]. This method allows us to trace the proportions of endophytic OTUs obtained from the initial samples subjected to surface sterilization across different decomposition periods (T1, T2, T3, and T4). Since the endophytic fungal OTUs in the initial living leaves were obtained through sequencing of surface-sterilized samples, these OTUs are regarded as the source of endophytic fungi in the leaf litter. The endophytic community from degrading litters for three treatments serve as the sinks for the endophytic microbe.

2.7.6. Structural Equation Modeling (SEM)

We employed piecewise structural equation modeling (piecewiseSEM) to evaluate the direct and indirect relationships among endophyte priority colonization, endophytic diversity, organic matter quality, degrading enzyme, and remaining mass. We initially constructed a prior model that included all hypothesized pathways and iteratively simplified the model by removing non-significant pathways until the final model was achieved. The suitability of the final model was evaluated utilizing Fisher's C statistic, as implemented in the piecewiseSEM package for R version 4.3.3 [62].

3. Results

3.1. Remaining Mass, CO_2 Release and Organic Matter Quality

This one-year incubation study revealed that the decomposition rates of leaf litter initially colonized by endophytic communities were markedly lower compared to those devoid of endophytes, with 52.0% and 43.7% of the initial mass remaining in the NS and SS treatments, respectively, versus only 20.3% in the IS treatment (Figure 1A; Table S1). The presence of epiphyllous microbes in the NS treatment resulted in a marginally lower decomposition rate when compared to the SS treatment, which lacked these microbes. Aligning with the final weight loss patterns of litter decomposition, CO_2 releases were the highest in the IS treatment and the lowest in the NS treatment (Figure 1B).

Index I exhibited an increasing trend along the direction of litter decomposition, indicating the enhancement of degradation intensity (Figure 1C; Table S1). In the initial stages, the degradation intensity of the IS treatment was lower compared to other treatments, while at the end of incubation, the mean value of the IS (2.29 ± 0.10) treatment was higher than that of the NS (2.02 ± 0.38) and SS (1.59 ± 0.06) treatments. Index II showed that, with the exception of the IS and NS treatments at T1 stage, its values generally display an increasing trend, suggesting that the accumulation of recalcitrance substances also increased as decomposition progresses (Figure 1D; Table S1). At the end of decomposition, the mean value of Index II for the IS treatment (1.30 ± 0.11) was also higher than the other two treatments (1.01 ± 0.08 for NS and 1.26 ± 0.11 for SS).

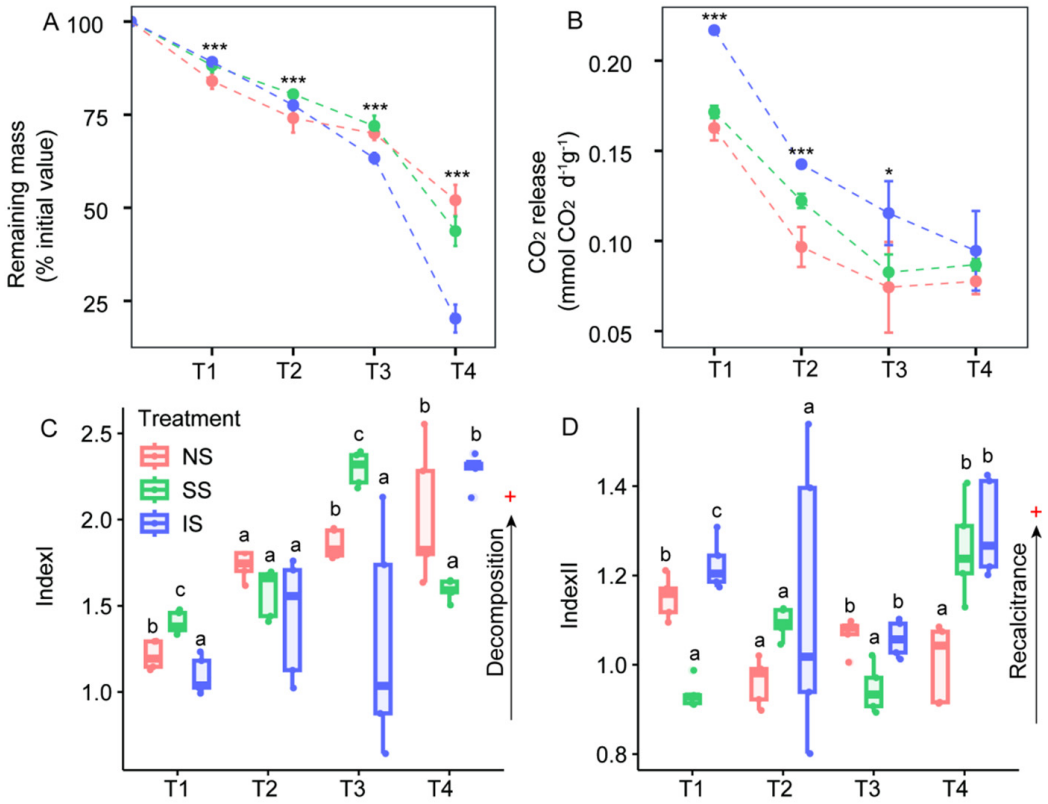

Figure 1. The differences in remaining mass (**A**), CO_2 release (**B**), decomposition degree (Index I, (**C**)), and recalcitrance (Index II, (**D**)) of leaf litter organic matter among the three treatments (natural state (NS, pink, surface sterilization (SS, green), and irradiation sterilization (IS, blue) during the four decomposition periods (T1, T2, T3, and T4). Asterisks and different lowercase letters indicate significant differences ($p < 0.05$, Duncan's test) among the three treatments.

3.2. Extracellular Enzyme Activity and Stoichiometry

The difference in extracellular enzyme activities between the three treatments along the incubation time is shown in Figure S1. The IS treatment showed significantly higher activities of cellulolytic enzymes (exocellulase, endocellulase and β-glucosidase) than the SS and NS treatments at T1 stage, and at later stages lower than the SS and NS treatments, in most cases (Figure S1A–C). NAG, LAP, and AP showed mixing pattern of difference among the three treatments along the incubation time (Figure S1D–F). Enzyme stoichiometry vectors during litter decomposition were characterized differently for different treatment (Figure 2A). Vector length and extracellular enzyme C/N and C/P ratios showed a declining pattern along the incubation direction, indicating a decline of microbial C limitation (Figure 2B,D,E). Vector angle and extracellular enzyme N/P showed, at the T1 stage, the SS treatment presented N limitation and, at later stages, the P limitation was observed for all treatments (Figure 2C,F). Along the direction of litter decomposition, the magnitude of differences in vector length and vector angle among the three treatments (IS, NS, and SS) decreased over time. At the T4 stage, the vector length of the IS treatment was significantly ($p < 0.05$) higher than that of the SS and NS treatments, while the vector angle is significantly ($p < 0.05$) lower than that of the SS and NS treatments (Figure 2B,C).

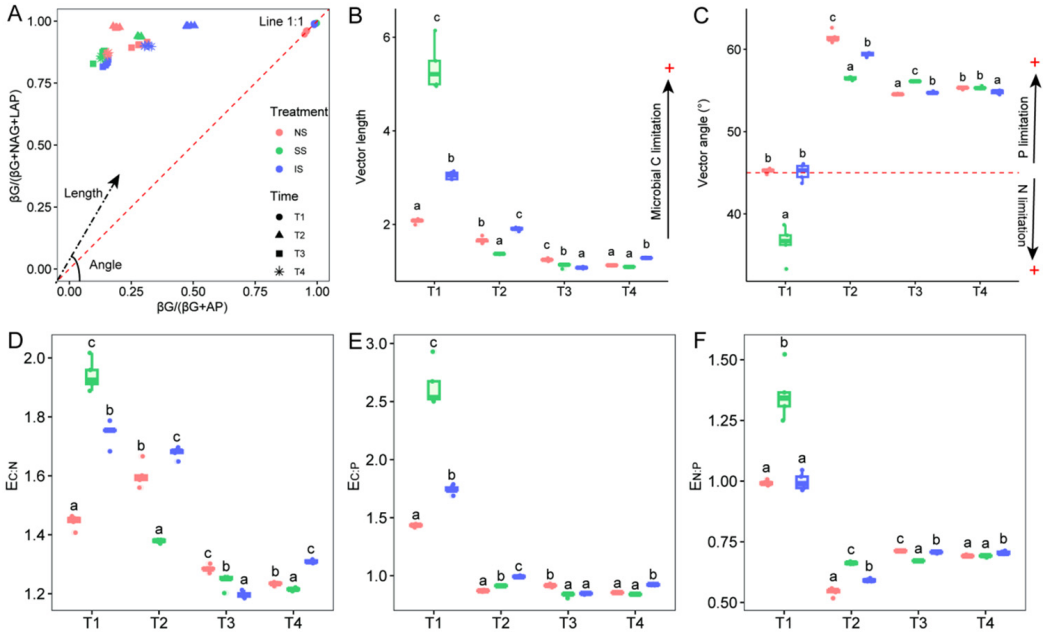

Figure 2. General principles of microbial C, N, and P metabolic limitations and stoichiometric characteristics of extracellular enzymes in leaf litter under three treatments (natural state (NS, pink), surface sterilization (SS, green), and irradiation sterilization (IS, blue)) during four decomposition periods (T1, T2, T3, and T4). (**A**), Enzyme vector model of extracellular enzyme stoichiometry; (**B**), Vector length; (**C**), Vector angle; (**D**), $E_{C:N}$ represents Ln(βG): Ln(NAG+LAP); (**E**), $E_{C:P}$ represents Ln(βG): Ln(AP); (**F**), $E_{N:P}$ represents Ln(NAG+LAP): Ln(AP); βG, β-1,4-Glucosidase; NAG, β-1,4-N-Acetylglucosaminidase; LAP, Leucine aminopeptidase; AP, Acid phosphatase. Different lowercase letters indicate significant differences ($p < 0.05$, Duncan's test) among different treatments.

3.3. Microbial Community Structure and Diversity

In the fungal communities, Ascomycota and Basidiomycota were the dominant phyla (Figure S2A). The fungal communities in newly fallen leaves (T0) at the phylum level show no significant differences between the NS and SS, whereas during the decomposition of litter, there are distinct differences in relative abundance at the phylum level among the three treatments. At the genus level, *Colpoma* was predominant at the most stages of litter decomposition (Figure S2B). By contrast, *Pilidium*, *Cylindrium*, *Mycena*, *Capnobotryella*, *Phialea*, and *Curvibasidium* were dominant only in one or a few specific stages of litter decomposition. Similar to the phylum level, there is little difference in the composition of fungal communities in newly fallen leaves between the SS and NS at the genus level. However, during the decomposition stage of the litter, the community composition exhibits significant differences among the three treatments.

Proteobacteria and Actinobacteriota were the dominant phyla in the bacterial communities (Figure S2C). The NS treatment showed significantly higher relative abundance in Actinobacteriota than the SS treatment in newly fallen leaves ($p < 0.05$; T0). In most cases, Proteobacteria showed an increased trend along the litter incubation time. At the genus level, no single genus was able to dominate in most instances, with the exception of Pseudomonas, which showed dominance at the T1 period (Figure S2D). There were no significant differences in relative abundance at the genus level between the NS and SS during the T0 period. However, along the trajectory of litter decomposition, the three treatments exhibited a noticeable variation in relative genus abundance.

The results of PCoA demonstrated that both fungal and bacterial communities in newly fallen leaves showed significant differences between the NS and SS treatments ($p < 0.05$; Figure 3A,C), indicating that there is a distinct difference in the composition of epiphytic and endophytic microbial communities in newly fallen leaves. During the

decomposition of litter, the IS, SS, and NS treatments also exhibited significant differences in the composition of fungal and bacterial communities ($p < 0.05$; Figure 3B,D).

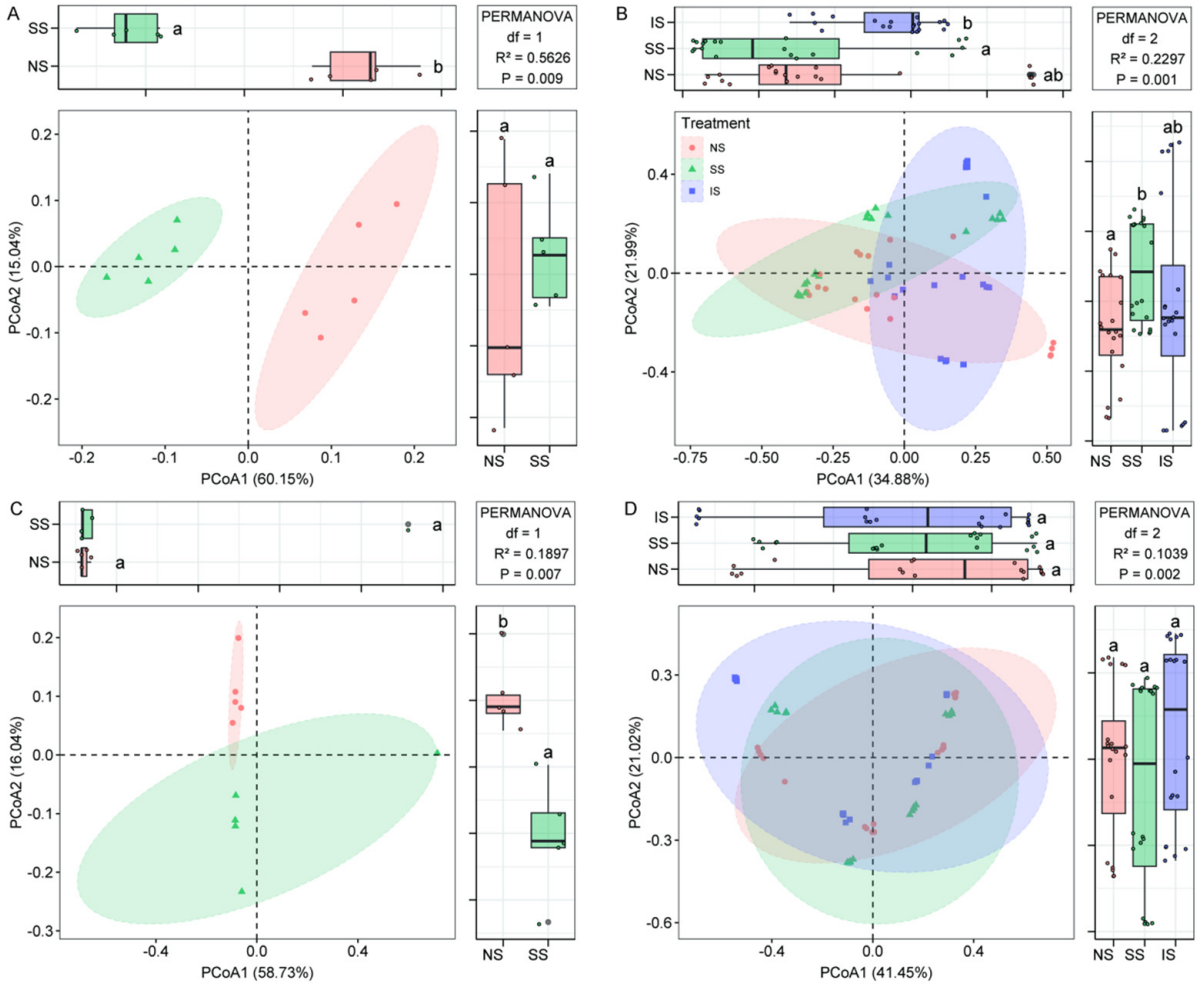

Figure 3. Principal coordinates analysis (PCoA) for fungal (**A**,**B**) and bacterial (**C**,**D**) communities at OTU level based on Bray–Curtis distance under three treatments (natural state (NS, pink), surface sterilization (SS, green), and irradiation sterilization (IS, blue)) at newly fallen leaf stages (**A**,**C**) and at litter decomposition stages (**B**,**D**). Different lowercase letters indicate significant differences among different treatments ($p < 0.05$, Adonis PERMANOVA).

Overall, along with the direction of litter decomposition, fungal alpha diversity tends to decrease, while bacterial alpha diversity tends to increase (Figure 4). In the IS treatment, fungal diversity reached its peak directly during the T1 stage, and was intermediate between the NS and SS, while bacterial diversity remained at its lowest at the T1 stage and was lower than both the NS and SS (Figure 4A,E). However, at the later stages of decomposition (T2, T3, and T4), alpha diversity did not show significant differences among the three treatments in most cases (Figure 4B–D,F–H).

The diversity trends of endophytic fungi and endophytic bacteria along the direction of litter decomposition are consistent with those of the overall fungal and bacterial communities (Figure 5). The patterns of diversity differences among the NS, SS, and IS treatments for endophytic microorganisms are also similar to those of the overall microbial diversity, suggesting that endophytes should be the important members in the overall microbial pool.

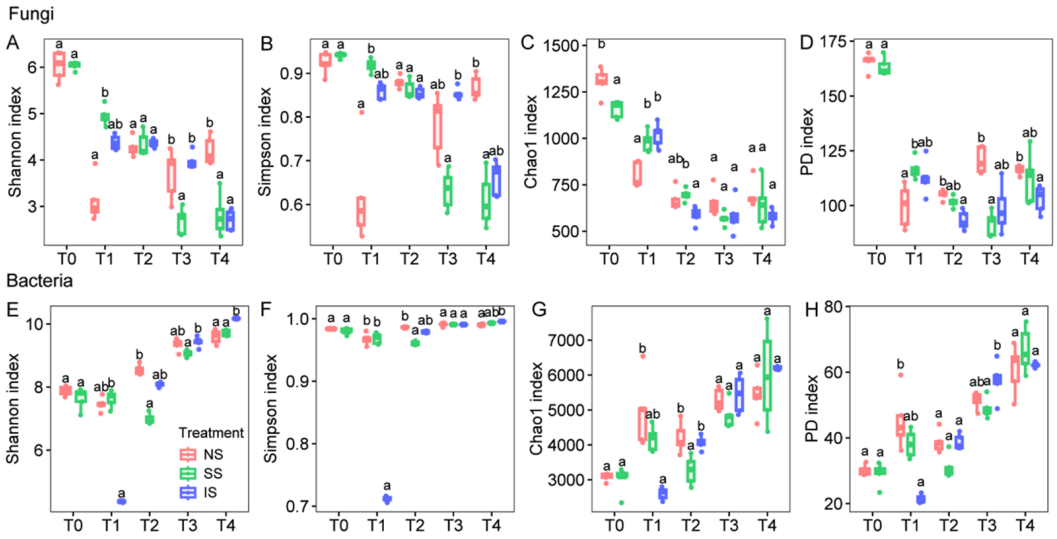

Figure 4. Changes in the alpha diversity of fungi (**A**–**D**) and bacteria (**E**–**H**) under the three treatments (natural state (NS, pink), surface sterilization (SS, green), and irradiation sterilization (IS, blue)) at newly fallen leaf stages (T0) and at litter decomposition stages (T1, T2, T3, and T4). Different lowercase letters indicate significant differences among different treatments ($p < 0.05$, Dunn's test).

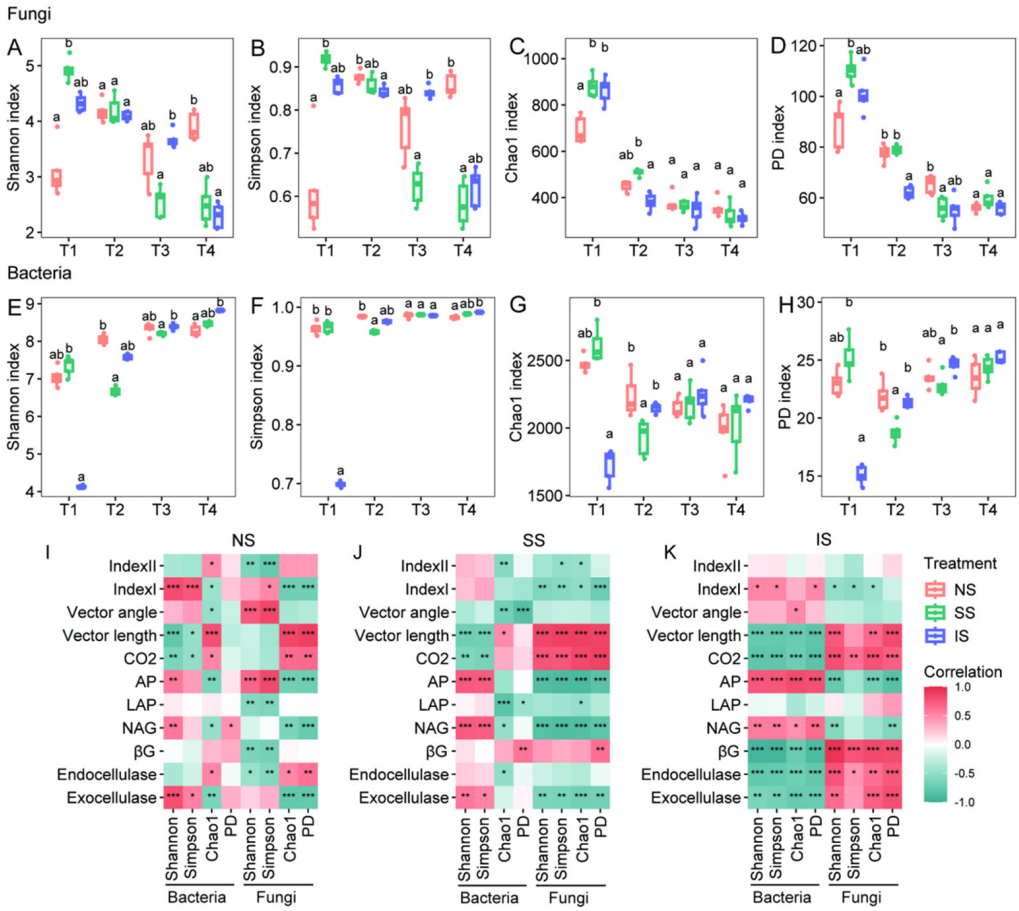

Figure 5. Changes in the alpha diversity of endophytic fungi (**A**–**D**) and endophytic bacteria (**E**–**H**) under the three treatments (natural state (NS, pink), surface sterilization (SS, green), and irradiation sterilization (IS, blue)) at newly fallen leaf stages (T0) and at litter decomposition stages (T1, T2, T3, and T4), as well as its correlation (**I**–**K**) with microbial decomposition functions. Different lowercase letters indicate significant differences among different treatments ($p < 0.05$, Dunn's test). Significance levels for each correlation are denoted as * $p < 0.05$, ** $p < 0.01$, *** $p < 0.001$.

Taking the endophytic microbial communities of surface-sterilized living leaves at the T0 stage of the SS treatment as a reference, a source tracking analysis of endophytic microbes was conducted (Figure 6). In most cases, from the early to the late stages of litter decomposition, endophytic microbes showed a decreasing trend. For instance, endophytic fungi at the end of incubation (T4) for the three treatments only accounted for 4.56% (NS), 2.68% (SS), and 2.49% (IS) of their original values; endophytic bacteria at the end of incubation only accounted for 15.62% (NS), 17.81% (SS), and 16.63% (IS) of their original values. Among them, endophytic bacteria in the IS treatment at the T1 stage only accounted for 12.25% of the initial number, which is mainly due to the endophytic microbes at the T1 stage of the IS treatment primarily originating from the soil microbial pool, due to the slower colonization rate; however, in later stages, the proportion of endophytic bacteria exceeds that of the T1 period due to the replenishment of the microbial pool. The differences in the reduction amplitude of endophytic microbes between different treatments are mainly at the T1 stage, with the SS treatment showing the smallest reduction (fungi retained 33.42%, and bacteria retained 42.28%), and the IS treatment showing the largest reduction (fungi retained 11.08%, and bacteria retained 12.25%). In subsequent decomposition stages, the proportion of endophytic microbes retained is not obviously different.

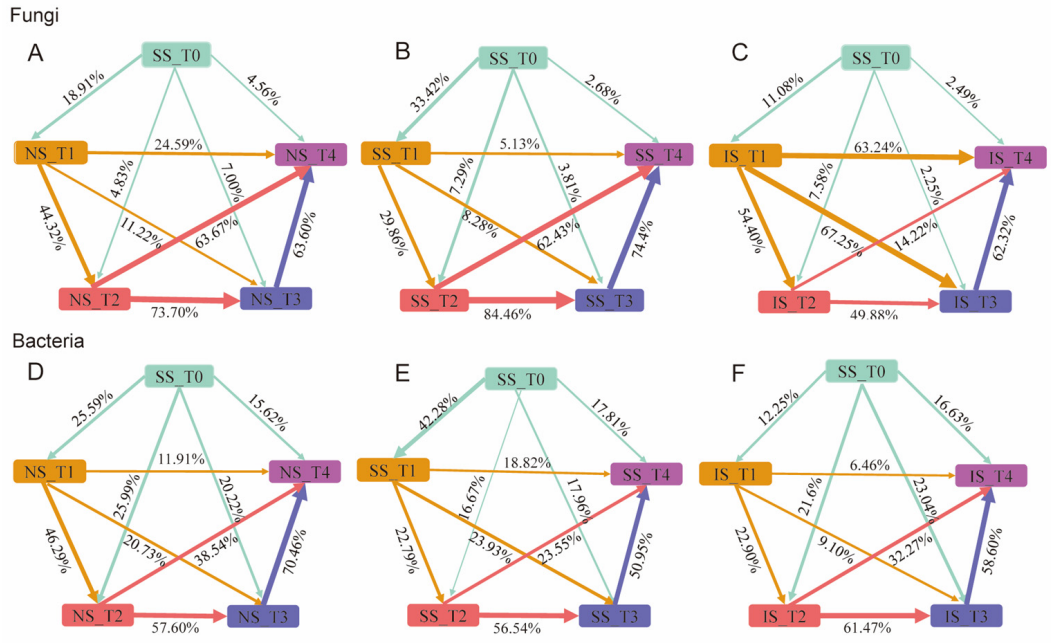

Figure 6. Source tracking analysis of endophytes ((**A**–**C**) for fungi; (**D**–**F**) for bacteria) during litter decomposition under three treatments (natural state (NS), surface sterilization (SS), and irradiation sterilization (IS)). SS_T0 represents the endophytes in litter treated with surface sterilization (SS) at newly fallen leaf stage (T0). T1, T2, T3, and T4 represent four different decomposition stages. The arrow points to a sink; otherwise, it indicates a source.

As is shown in Figure S3, 16 fungal and 20 bacterial clades present statistically significant differences between the three treatments with LDA threshold of 3.0 (Figure S3A,C). For fungi, Helotiales (order), *Pilidium* (genus), Chaetomellaceae (family), and *Pilidium anglicum* (species) showed more abundant advantage in the IS treatment group, while Sordariomycetes (class), *Cylindrium* (genus), and Hypocreales (order) were the most abundant in the NS treatment (Figure S3B). For bacteria, *Burkholderia–Caballeronia–Paraburkholderia* (genus), *Caballeronia sordidicola* (species), Acetobacterales (order), Acetobacteraceae (family), and Beijerinckiaceae (family) in the SS treatment presented the most relative abundance among the three treatment, while Bacteroidota (phylum), Bacteroidia (class), Micromonosporales (order), Micromonosporaeae (family), Flavobacteriales (order), *Actino-*

planes (genus), Bdellovibrionota (phylum), *Micromonospora* (genus), and Alcaligenaceae (family) in the IS treatment was the most abundant (Figure S3D).

3.4. Co-Occurrence Network Analysis

Microbial co-occurrence networks are depicted in Figure 7. During the symbiotic phase, the microbial networks are relatively simple and modularly uniform (Figure 7A,B,F,G). However, during the decomposition phase of litter, the networks under the three treatments become more complex, and the modules no longer exhibit uniform distribution (Figure 7C–E,H–J). Figure S4 illustrates the composition of the top four network modules of fungi and bacteria at the genus level during the symbiotic and saprotrophic stages. Some members that composed the modules during the symbiotic phase remain as important members of the modules during the saprotrophic phase. For instance, the fungal genera *Colpoma* and *Phialea*, from the symbiotic phase in the NS treatment, still became important members of the modules in the saprotrophic phase (Figure S4A,C–E); the genera *Cylindrium*, *Curvibasidium*, and *Phialea*, from the symbiotic phase in the SS treatment, also became members of the network modules in the saprotrophic phase (Figure S4B–E). The bacterial genera *Burkholderia–Caballeronia–Paraburkholderia* and *Sphingomonas* under the NS and SS treatments were important components of the network modules in the saprotrophic phase (Figure S4F–J). For the fungal network modules, the three treatments only shared *Cylindrium*, *Phialea*, and *Colpoma* as three important constituent members, with significant differences in overall module composition (Figure S4C–E). For the bacterial network modules, the three treatments shared a greater number of genera, including *Luteibacter*, *Pseudomonas*, *Bradyrhizobium*, *Burkholderia–Caballeronia–Paraburkholderia*, and *Sphingomonas*, but their relative abundances differed markedly between different modules (Figure S4H–J).

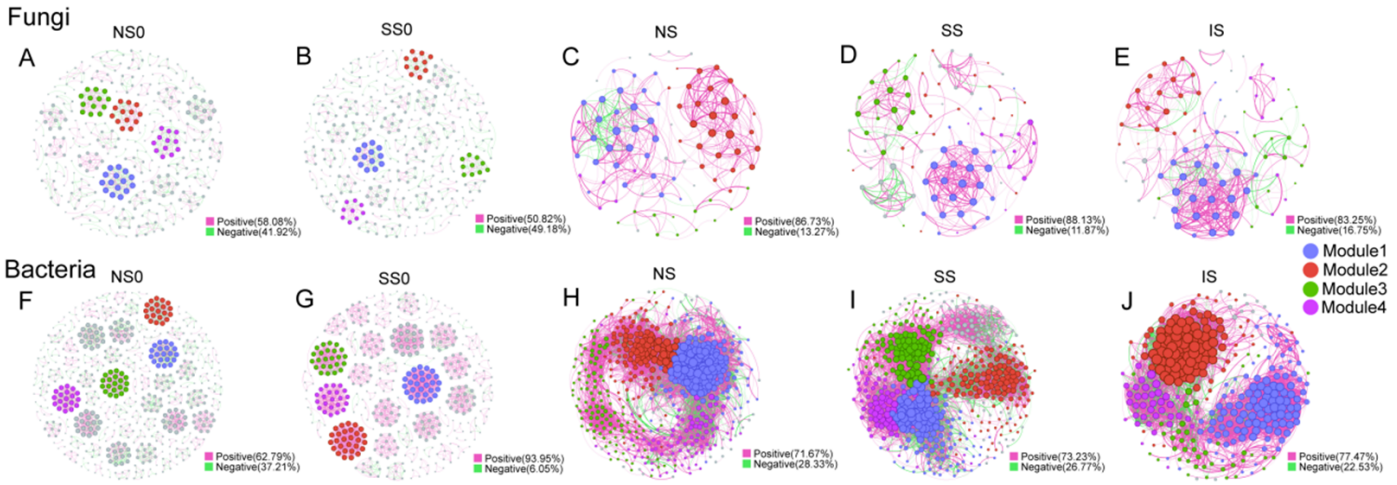

Figure 7. Microbial co-occurrence networks under three treatments (natural state (NS), surface sterilization (SS), and irradiation sterilization (IS)) at newly fallen leaf stages ((**A**,**B**) for fungi; (**F**,**G**) for bacteria) and at litter decomposition stages ((**C**–**E**) for fungi; (**H**–**J**) for bacteria).

Based on within-module connectivity and between-module connectivity, a total of 3 fungal and 13 bacterial keystone taxa were identified (Figure 8; Table S2). Notably, only OTU_2565 is not of endophytic origin; the other 15 species are exclusively derived from the endophytic community. Among these 15 species, OTU_409 is exclusively derived from the SS treatment, while the other 14 species are present across all three treatments (Figure 8).

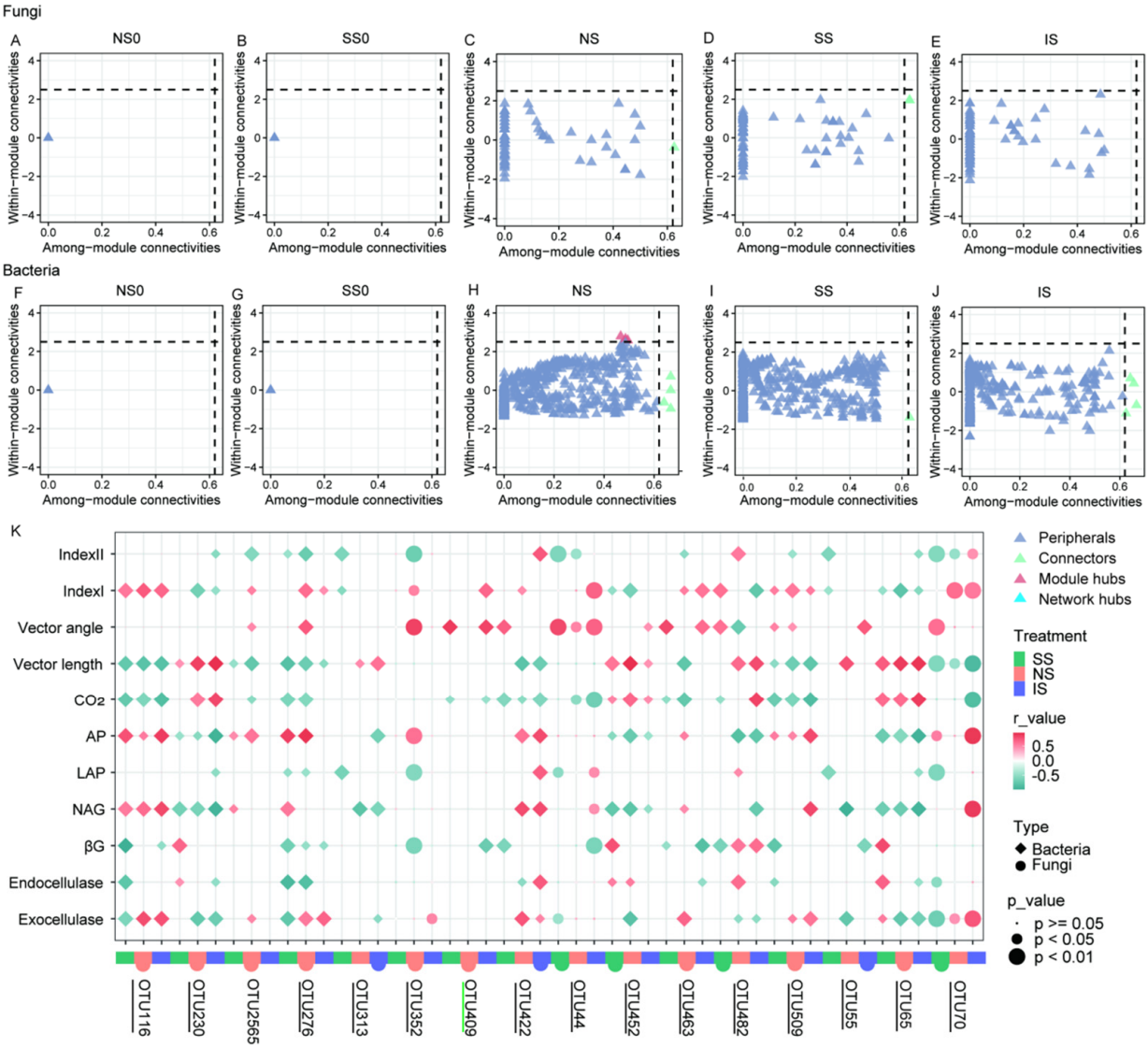

Figure 8. Keystone taxa identified through network analysis ((**A**–**E**) for fungi and (**F**–**J**) for bacteria) and their correlations (**K**) with decomposition functions under three treatments (natural state (NS), surface sterilization (SS), and irradiation sterilization (IS)). Black lines signify that these OTUs are keystone endophytes present across the NS, SS, and IS treatment groups, while green line indicates their presence specifically in the SS treatment group. The colored semicircles on the *x*-axis represent the treatment groups to which each OTU belongs, with different colors indicating different groups. See Figure 2 for the abbreviations.

3.5. Community Assembly

For both fungi and bacteria, the absolute values of almost all βNTI values at each litter decomposition stage were less than 2, indicating that the community assembly of both fungi and bacteria was predominantly driven by stochastic processes (i.e., the sum of undominated and homogenizing dispersal) (Figure 9A,C). Among these, homogenizing dispersal, determined by RCI values, accounted for a very small proportion, only appearing in the community assembly of fungi in the SS (2.5%) and IS (5%) treatments (Figure 9B,D). Deterministic processes (heterogeneous selection) played a minor role in community assembly, with the proportions in the three treatments being, for fungi, NS (12.5%) > SS (7.5%) > IS (5%), and for bacteria, NS (12.5%) > SS (10%) > IS (2.5%) (Figure 9E–J).

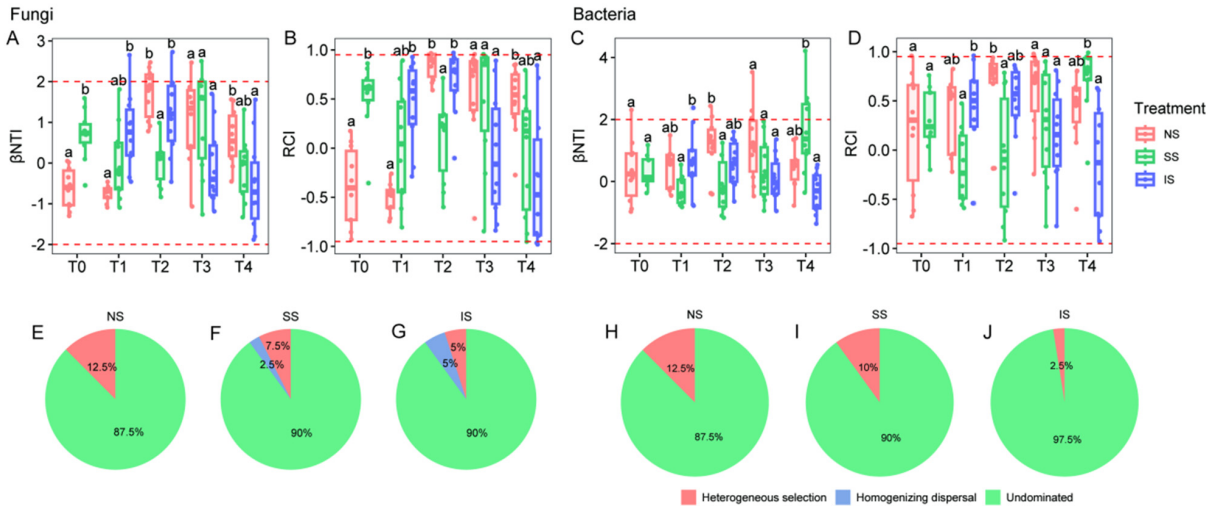

Figure 9. Microbial community assembly ((**A**,**B**,**E**–**G**) for fungi; (**C**,**D**,**H**–**J**) for bacteria) under three treatments (natural state (NS, pink), surface sterilization (SS, green), and irradiation sterilization (IS, blue)) at newly fallen leaf stages (T0) and at litter decomposition stages (T1, T2, T3, and T4). Different lowercase letters indicate significant differences among different treatments ($p < 0.05$, Dunn's test).

3.6. Relationship of Endophytes to Decomposition Function

Figure 5I–K reveal inconsistent correlations between endophytic fungi and bacteria and various functional variables across three treatments, indicating that the initial establishment of endophytic microbial colonization influences their functional roles. For the exocellulase enzyme, significant positive correlations with bacterial diversity and significant negative correlations with fungal diversity were observed in the NS and SS treatments. By contrast, in the IS treatment, bacterial diversity showed a significantly negative correlation, while fungal diversity showed a significantly positive correlation with cellulases. Endophytic bacterial diversity predominantly exhibited positive correlations with NAG enzyme activity, which is related to nitrogen metabolism, whereas endophytic fungal diversity showed negative correlations with the NAG enzyme; in most cases, the diversity of endogenous microbes was not significantly correlated with LAP enzyme activity. For the AP enzyme associated with phosphorus release, endogenous bacterial diversity was mostly positively correlated, while endophytic fungal diversity was negatively correlated. Regarding CO_2, endophytic bacterial diversity was negatively correlated, whereas endophytic fungal diversity was positively correlated. For vector length, endophytic bacterial diversity was negatively correlated, and endophytic fungal diversity was positively correlated, suggesting that endogenous microbial diversity is closely related to carbon metabolism. However, in most cases, the correlation between endogenous microbial diversity and vector angle was not significant, indicating that endogenous microbial diversity is not closely related to nitrogen and phosphorus resources. In most cases, endogenous bacterial diversity was positively correlated with Index I, while fungal diversity was negatively correlated, indicating that endogenous microbes affect the degree of litter decomposition. However, in most cases, it was not significantly correlated with Index II. The correlation diagram of endogenous microbes and functions indicates the sustainability of endogenous microbes in terms of functional performance.

Figure 8K highlights the relationships of 16 keystone microbes (15 taxa belonging to endophytes), such as OTU_70 (fungi), OTU_65 (bacteria), OTU_509 (bacteria), OTU_482 (bacteria), OTU_452 (bacteria), and OTU_422 (bacteria), with decomposition functions, revealing significant positive or negative correlations in most instances. This indicated a substantial association between the abundance of these microbes and the decomposition processes. The varying correlations across different treatments implied that the initial

microbial colonization patterns significantly influenced the relationship between endogenous microbes and their functional roles in decomposition. In general, keystone microbes tend to show positive correlations with the vector angle, suggesting their potential role in phosphorus limitation. The majority of these microbes correlated positively with Index I, which may indicate their contribution to enhancing litter decomposition. Conversely, a negative correlation with Index II was observed, hinting at their possible role in diminishing litter antagonism. Regarding other decomposition function indicators, these keystone microbes did not exhibit a uniform pattern; instead, their effects varied among different microbial species and treatments, underscoring the complexity of microbial influence on decomposition dynamics.

In this study, we delved into the causal interconnections among various variables shaped by the priority colonization of endophytic microbial communities throughout four distinct phases of litter decomposition. The structural equation models (SEMs, Figure 10) clarified the temporal effects of endophytic priority colonization on endophytic diversity, decomposition degree (Index I), remaining mass, and the enzymatic activities of β-glucosidase and exocellulase. During the initial phase (T1), priority colonization of endophytic microbial communities significantly enhanced the diversity of endophytic bacteria but markedly reduced that of endophytic fungi, with the reverse pattern observed in the final phase (T4). The priority colonization showed a significantly negative impact on the remaining mass in the early stages (T1 and T2), thereby promoting litter decomposition, but this effect was reversed in the later stages (T3 and T4), significantly inhibiting decomposition. The Index I, which characterizes the decomposition degree based on the infrared absorption bands of functional groups, did not show a significant association with initial treatments in most periods, with the exception of the T3 phase. Endophytic bacteria and fungi continuously influenced decomposition functions, exerting varying effects on the decomposition degree, remaining mass, β-glucosidase, and exocellulase across different stages. Endophytic bacterial diversity had a significantly negative correlation with the remaining mass in most periods, promoting litter decomposition, while endophytic fungi only showed a significant negative correlation with the remaining mass during the T3 phase. Endophytic bacterial diversity did not significantly affect the decomposition degree in the early stages (T1 and T2) but had a substantial impact in the later stages (T3 and T4). By contrast, endophytic fungi significantly influenced the decomposition degree in both the initial (T1) and final (T4) phases. The SEMs also revealed that endophytic microbial diversity had significant positive or negative effects on degrading enzymes. These findings suggest that the interaction between endophytic microbial communities and their environment is intricate, and their influence on litter decomposition is contingent on specific contexts and sensitive to timing.

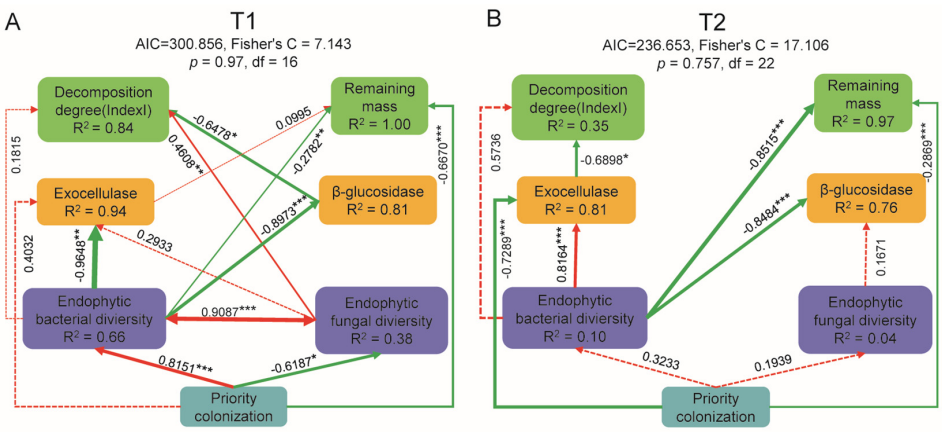

Figure 10. *Cont.*

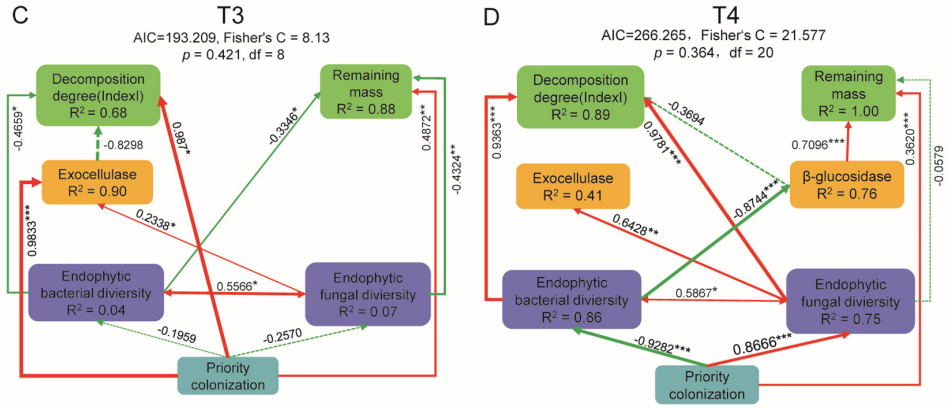

Figure 10. The piecewise structural equation model ((**A**) T1; (**B**) T2; (**C**) T3; (**D**) T4) of analyzing the causal relationship between the variables at different stages of litter decomposition. Double-headed arrows indicate correlations between variables, while single-headed arrows denote causal relationships. The color of the lines signifies positive effects (red) and negative effects (green), and the solidness of the lines indicates significant (solid line) and non-significant (dashed line) relationships. The values on the lines represent standardized path coefficients. Significance levels for each predictor are denoted as * $p < 0.05$, ** $p < 0.01$, *** $p < 0.001$.

4. Discussion

4.1. Litter Decomposition

Our findings reveal that the initial establishment of endophytic microbial communities significantly suppresses litter decomposition, reducing the mass loss from 80% to 46%, which is consistent with our initial hypothesis. The suppressive effect of endophyte-colonized decomposition is a phenomenon also observed in other leaf litter species across terrestrial ecosystems [3,63–65]. The decomposition degree (Index I), assessed through infrared absorption band analysis, demonstrated that endophytic priority colonization mitigated the decomposition of oak leaf litter. Drawing from the information on the infrared absorption band, we speculate that endophytic colonization may potentially decelerate the breakdown of labile components, including aliphatic C-H groups [66].

Furthermore, an enzyme stoichiometry-based resource limitation analysis reveals that during the later stages of decomposition, phosphorus limitation significantly constrains the process. This phosphorus limitation is slightly more pronounced in the presence of endophytic colonization compared to treatments without endophytes. Since phosphorus limitation is a critical factor impacting litter decomposition, it is reasonable to deduce that the phosphorus limitation enhanced by endophytic microbial colonization is a major contributor to the observed slower decomposition rate in the colonized treatment group [67–69]. The comparative analysis of mass loss between the natural leaves with epiphyllous microbe and the surface-sterilized leaves, which allow only endophytic colonization, shows no significant differences throughout most phases of litter decomposition. This result indicates that the presence of epiphyllous microbes has a minimal effect on the influence of endophytic microbial colonization on the rate of decomposition [70].

4.2. Microbial Diversity

The preferential colonization by endophytic microbial communities resulted in variable patterns of fungal and bacterial diversity across the majority of decomposition stages, with these variations being statistically non-significant in most instances. This implies that the diversity of microbial decomposers throughout the litter decomposition process is influenced not only by the initial colonization of endophytic microbes but potentially by the local species pool of microbes. This indicates a dynamic interplay between the historical colonization events of endophytes and the local microbial species pool, which shapes

the progression of litter decomposition [7,34]. Nevertheless, LEfSe analysis reveals that priority colonization by endophytic microbes influences certain microbial taxa at various taxonomic levels. Among fungi, the priority colonization of endophytes exerts a significant inhibitory effect on taxa such as Helotiales (order), *Pilidium* (genus), Chaetomellaceae (family), Pilidium anglicum (species), Sordariomycetes (class), *Cylindrium* (genus), Hypocreales (order), and *Cylindrium* sp. (species). By contrast, for bacteria, the priority colonization by endophytes notably favors taxa such as *Burkholderia-Caballeronia-Paraburkholderia* (genus), *Caballeronia sordidicola* (species), Acetobacterales (order), Acetobacteraceae (family), and Beijerinckiaceae (family). This finding indicates that the establishment of endophytic microbial communities can have either positive or negative impacts on different microbial taxa at various taxonomic levels, suggesting that endophytic colonization may lead to niche differentiation within microbial decomposer communities [15,64].

Source tracking analysis of endophytic microbes during the litter decomposition process, with the initial endophytic microbial community as a reference, indicates a clear downward trend in endophytic numbers, which is consistent with expectations. This is likely because most endophytic species do not persist into the later stages of decomposition due to their limited ability or inability to utilize litter [19,20,26]. Throughout this process, endophytic fungal species exhibit a more rapid decline compared to endophytic bacterial species, implying that endophytic bacteria, in general, possess greater adaptability to the litter decomposition process than endophytic fungi [71]. Contrasting the downward trend in endophytic fungal diversity with the progression of litter decomposition, there is a notable upward trend in endophytic bacterial diversity, even as species numbers decrease. We speculate that the differences in resource utilization capabilities between endophytic fungi and bacteria are most likely the dominant factor influencing the distinct changes in their respective communities. Compared to endophytic fungi, endophytic bacteria are more adept at utilizing high-quality and easily decomposable organic substances in oak leaf litter and have a faster reproduction rate, enabling them to more effectively occupy the ecological niches in litter [65]. Therefore, we can artificially introduce specific endophytic bacteria for regulating the balance between endophytic bacteria and fungi, which can modulate the rate of soil organic matter decomposition. This approach holds significant ecological implications for the management of forest ecosystems, particularly for the restoration of soils in degraded ecosystems. In treatments where irradiation sterilization is applied, endophytic microbes are observed to emerge during the decomposition process, predominantly sourced from the surrounding species pool. Furthermore, during the initial phases of decomposition, the rate of colonization by endogenous bacteria is markedly slower compared to that of endogenous fungi. This disparity may be attributed to the distinct transmission modes, with fungi being able to utilize aerial spores for rapid dispersal via wind or catapult mechanisms [72].

4.3. Microbial Co-Occurrence Network and Community Assembly

The network modules elucidate the intimate associations among microbial groups, thereby characterizing, to a certain extent, the functional guilds within microbial communities [73]. Taxa that are present in the modules during the endophytic phase continue to be significant constituents in the modules during the saprotrophic phase. Notable examples include the fungal genera *Cylindrium*, *Curvibasidium*, and *Phialea*, as well as the bacterial genera *Burkholderia–Caballeronia–Paraburkholderia* and *Sphingomonas*. This suggests that these microbial guilds from the endophytic phase may play a significant role in litter decomposition. The pioneer effect of endophytic microbes also leads to the differentiation of functional modules within the microbial network. For fungal network modules, the three treatments only share *Cylindrium*, *Phialea*, and *Colpoma*, still exhibiting considerable

differentiation overall. However, for bacterial network modules, the three treatments share a greater number of taxa, including *Luteibacter*, *Pseudomonas*, *Bradyrhizobium*, *Burkholderia–Caballeronia–Paraburkholderia*, and *Sphingomonas*, yet even so, their relative abundances still show considerable differentiation among different treatments. This suggests that the historical colonization event by endophytic microbial communities has resulted in alterations to species interactions within these communities [7]. Collectively, the priority colonization by endophytic microbial communities appears to exert a more pronounced influence on the functional guilds of fungi than on those of bacteria during the saprotrophic phase.

Concurrently, our analysis of the microbial network has revealed a total of 16 keystone species, with the notable exception of one that is not of endogenous origin. This underscores the pivotal role that endogenous microbes play in shaping species interactions within the saprotrophic microbial community. This prominence can be interpreted as an expression of the priority effect, suggesting that the initial colonization by endophytes significantly dictates the subsequent species interactions within the microbial community throughout the decomposition process [7]. Among the 15 endogenous keystone microbes identified, 3 are fungi and 12 are bacteria, which suggests that, within the endogenous microbial community, bacteria likely exert a more substantial influence on species interactions than fungi. This observation aligns with the above-mentioned higher retention proportion of endophytic bacteria compared to endophytic fungi during the decomposition process, thereby reinforcing this viewpoint.

During the decomposition of litter, interactions among the colonizing microbial community take place, which to some extent reflect the process of community assembly. The priority colonization by endophytic microbes, a notable historical event in assembly, can exert significant influences on subsequent microbial succession and the assembly of the community. Our study demonstrates that the deterministic processes resulting from the priority colonization of endophytic microbial communities constitute a larger proportion in community assembly than those in the absence of initial endophytic colonization. This finding implies that endophytes exert a certain selective pressure on the subsequent assembly of microbial communities during the decomposition of litter. Nevertheless, the comprehensive analysis of community assembly reveals that the deterministic processes account for a minor proportion, regardless of the presence or absence of endophytic colonization, with the maximum proportion not exceeding 15%. Instead, stochastic processes predominantly govern the overall community assembly dynamics. It is widely accepted that resource abundance is a critical factor enhancing stochasticity in ecological processes [74–76]. An analysis of extracellular enzyme stoichiometry indicates that carbon resources are plentiful for the majority of the decomposition period. This abundance of carbon resources affords members of the local microbial community the opportunity for stochastic colonization of litter, thereby enabling their influence to potentially override the effects of the initial endophytic colonization event.

4.4. Enduring Effect of Endophytic Microbe on Litter Decomposition

At the diversity level, endophytic fungi and bacteria are closely linked to decomposition functions. Regardless of whether the degradation rate is calculated from mass loss, or the degree of decomposition is determined by organic carbon functional groups, endophytic bacteria typically facilitate litter decomposition, whereas endophytic fungi generally have an inhibitory effect. Both endophytic bacteria and fungi display significant positive or negative correlations with cellulase activity, potentially influencing the role of endophytic microbial diversity in decomposition processes. Additionally, endophytic fungi and bacteria are closely associated with vector length, suggesting their active involvement in carbon (C) metabolic processes. Endophytic bacteria exhibit positive correlations

with β-N-acetylglucosaminidase and acid phosphatase activities, indicating a probable involvement in the metabolism of nitrogen and phosphorus.

At the mono-species level, we have identified a significant correlation between keystone endophytic microbes and their roles in decomposition processes. A majority of these microbes, including *Chalara aurea* (OTU_70, fungi), *Dactylaria purpurella* (OTU_44, fungi), *Idriellopsis uncinospora* (OTU_352, fungi), *Caulobacter* sp. (OTU_509, bacteria), *Asticcacaulis* (OTU_463 and OTU_409, bacteria), *Flavobacterium* (OTU_422, bacteria), *Sphingomonas* (OTU_276, bacteria), and *Reyranella* (OTU_116, bacteria), exhibit a positive correlation with the decomposition degree (Index I). This suggests that these keystone microbes are instrumental in the decomposition of litter. Moreover, some of these microbes, such as *Dactylaria purpurella* and *Chalara aurea*, though known to inhabit litter or decaying wood, have not been systematically characterized in terms of their roles in microbial networks or decomposition functions [77,78]. The genus *Flavobacterium*, prominent on wheat leaves and roots as a keystone endophytic microbe, and the most connected genus in the microbial network [79], has not been previously implicated in litter decomposition. In microbial co-occurrence network analysis, the interactions between keystone microbes and overall microbial functions range from synergistic to antagonistic. It is widely accepted that, in resource-limited environments, microbes may compete for the same resources, leading to antagonistic relationships; by contrast, abundant resources may foster synergistic interactions among different microbes [80–83]. Given the absence of a carbon resource limitation along the decomposition gradient, it is likely that keystone microbes and other decomposers engage in synergistic relationships during the decomposition process. This synergism is consistent with the observed positive association between keystone microbes and the decomposition degree (Index I).

5. Conclusions

The findings of this study indicate that endophytic communities exert a retarding effect on litter decomposition in oak forests. Given that oak leaves are of high quality, they tend to decompose rapidly the following summer, driven by the high temperatures and heavy rainfall characteristics of subtropical regions. This rapid decomposition also leads to a swift loss of nutrients, which is detrimental to the development of oak forest vegetation. Consequently, the preferential colonization by endophytic microbes effectively acts as a nutrient slow-release mechanism, conducive to the formation of soil organic matter. Therefore, understanding this process is of significant ecological importance for the conservation and management of soil ecosystems in oak forests.

This study also reveals a notable persistence of endophytic bacteria throughout the decomposition, suggesting a higher adaptability to the decomposing environment compared to endophytic fungi. Furthermore, the identification of keystone species originated from endophytes within the microbial network underscores their influence on overall community function and decomposition degree. The positive correlation between these endophytic keystone species and decomposition functions highlights their synergistic role. The enduring effects of endophytic microbes on community assembly and function contribute to a deeper understanding of the microbial mediation of decomposition dynamics.

Supplementary Materials: The following supporting information can be downloaded at: https://www.mdpi.com/article/10.3390/f16020249/s1, Figure S1: Extracellular enzyme activity in the litter decomposition process (T1, T2, T3, and T4) under three treatments (natural state (NS, orange), surface sterilization (SS, green), and irradiation sterilization (IS, purple)). βG, β-1,4-glucosidase; NAG, β-1,4-N-acetylglucosaminidase; LAP, leucine aminopeptidase; AP, acid phosphatase. * and ** indicate statistical significance at the $p < 0.05$ and $p < 0.01$ levels (Duncan's test), respectively; Figure S2: Fungal and bacterial species composition in litter under three treatments (natural state

(NS), surface sterilization (SS), and irradiation sterilization (IS)) at newly-fallen leaf stages (initial period T0) and at litter decomposition stages (T1, T2, T3, and T4). The changes in relative abundance of the top 10 fungal communities at the phylum level (A) and genus level (B). The changes in relative abundance of the top 10 bacterial communities at the phylum level (C) and genus level (D); Figure S3: LEfSe analysis of microbial communities in litter under three treatments (natural state (NS, orange), surface sterilization (SS, green), and irradiation sterilization (IS, purple)). Histogram of the LDA scores computed for features differentially abundant between litter treated with natural state, surface sterilization, and irradiation sterilization for fungi (A) and bacteria (B). Histogram of the relative abundance of the top 10 features by LDA value for fungi (B) and bacteria (D) in litter under three treatments; Figure S4: Species composition within network modules of fungal and bacterial communities. The figure shows the relative abundance of the top 10 OTUs at the genus level within the top four modules in litter under three treatments (natural state (NS, orange), surface sterilization (SS, green), and irradiation sterilization (IS, purple)); Table S1: The indices relative to litter decomposition at different stages (T1, T2, T3, and T4) under three treatments (NS, SS, and IS); Table S2: The list of keystone taxa identified through network analysis under three treatments (natural state (NS), surface sterilization (SS), and irradiation sterilization (IS)).

Author Contributions: Conceptualization, X.H. and D.Y.; methodology, X.H. and D.Y.; software, D.Y. and Y.L.; validation, Y.L. and Z.H.; formal analysis, X.H., D.Y., and Y.L.; investigation, D.Y. and Z.H.; resources, X.H.; data curation, D.Y. and Y.L.; writing—original draft preparation, X.H. and D.Y.; writing—review and editing, X.H., Z.H., and X.K.; visualization, D.Y.; supervision, X.H. and Y.L.; projection administration, X.H. and Y.L.; funding acquisition, X.H., Y.L., Z.H., and X.K. All authors have read and agreed to the published version of the manuscript.

Funding: This work was supported by the National Natural Science Foundation of China (Grant numbers 32060332, 31670624, and 32160356) and the General Program of Scientific Research Foundation of Hunan Provincial Education Department (22C0278) and the Youth Program of Scientific Research Foundation of Hunan Provincial Education Department (24B0500).

Data Availability Statement: The datasets in this study are available from Supplementary Tables S1 and S2, and Figures S1–S4.

Conflicts of Interest: The authors declare no conflicts of interest.

References

1. Ball, B.A.; Carrillo, Y.; Molina, M. The influence of litter composition across the litter-soil interface on mass loss, nitrogen dynamics and the decomposer community. *Soil Biol. Biochem.* **2014**, *69*, 71–82. [CrossRef]
2. Rachmawati, S.; Yulistyarini, T.; Hairiah, K. Decomposition of tree litter: Interaction between inherent quality and environment. *Biodiversitas* **2019**, *20*, 1946–1952. [CrossRef]
3. Siegrist, J.A.; McCulley, R.L.; Bush, L.P.; Phillips, T.D. Alkaloids may not be responsible for endophyte-associated reductions in tall fescue decomposition rates. *Funct. Ecol.* **2010**, *24*, 460–468. [CrossRef]
4. Wolfe, E.R.; Ballhorn, D.J. Do foliar endophytes matter in litter decomposition? *Microorganisms* **2020**, *8*, 446. [CrossRef]
5. Sun, X.; Zheng, Y.; Xu, G.; Guo, Q.; Tan, J.; Ding, G. Fungal diversity within the phyllosphere of *Pinus massoniana* and the possible involvement of phyllospheric fungi in litter decomposition. *Fungal Biol.* **2021**, *125*, 785–795. [CrossRef] [PubMed]
6. Chen, Y.; Wang, H.; Li, L.; Dai, C. The potential application of the endophyte *Phomopsis liquidambari* to the ecological remediation of long-term cropping soil. *Appl. Soil Ecol.* **2013**, *67*, 20–26. [CrossRef]
7. Lin, Y.; He, X.; Ma, T.; Han, G.; Xiang, C. Priority colonization of *Cinnamomum camphora* litter by endophytes affects decomposition rate, fungal community and microbial activities under field conditions. *Pedobiologia* **2015**, *58*, 177–185. [CrossRef]
8. Mustonen, K.; Mykrä, H.; Louhi, P.; Markkola, A.; Tolkkinen, M.; Huusko, A.; Alioravainen, N.; Lehtinen, S.; Muotka, T. Sediments and flow have mainly independent effects on multitrophic stream communities and ecosystem functions. *Ecol. Appl.* **2016**, *26*, 2116–2129. [CrossRef] [PubMed]
9. Bell-Dereske, L.; Gao, X.; Masiello, C.A.; Sinsabaugh, R.L.; Emery, S.M.; Rudgers, J.A. Plant–fungal symbiosis affects litter decomposition during primary succession. *Oikos* **2017**, *126*, 801–811. [CrossRef]
10. Sun, K.; Cao, W.; Hu, L.; Fu, W.; Gong, J.; Kang, N.; Dai, C. Symbiotic fungal endophyte *Phomopsis liquidambari-rice* system promotes nitrogen transformation by influencing below-ground straw decomposition in paddy soil. *J. Appl. Microbiol.* **2019**, *126*, 191–203. [CrossRef] [PubMed]

11. Wolfe, E.R.; Younginger, B.S.; LeRoy, C.J. Fungal endophyte-infected leaf litter alters in-stream microbial communities and negatively influences aquatic fungal sporulation. *Oikos* **2019**, *128*, 405–415. [CrossRef]
12. Korkama-Rajala, T.; Müller, M.M.; Pennanen, T. Decomposition and fungi of needle litter from slow- and fast-growing Norway spruce (*Picea abies*) clones. *Microb. Ecol.* **2008**, *56*, 76–89. [CrossRef] [PubMed]
13. Grimmett, I.J.; Smith, K.A.; Bärlocher, F. Tar-spot infection delays fungal colonization and decomposition of maple leaves. *Freshw. Sci.* **2012**, *31*, 1088–1095. [CrossRef]
14. Omacini, M.; Semmartin, M.; Pérez, L.I.; Gundel, P.E. Grass–endophyte symbiosis: A neglected aboveground interaction with multiple belowground consequences. *Appl. Soil Ecol.* **2012**, *61*, 273–279. [CrossRef]
15. Gundel, P.E.; Helander, M.; Garibaldi, L.A.; Vázquez-de-Aldana, B.R.; Zabalgogeazcoa, I.; Saikkonen, K. Role of foliar fungal endophytes in litter decomposition among species and population origins. *Fungal Ecol.* **2016**, *21*, 50–56. [CrossRef]
16. Gundel, P.E.; Helander, M.; Garibaldi, L.A.; Vázquez-de-Aldana, B.R.; Zabalgogeazcoa, I.; Saikkonen, K. Direct and indirect effects of the fungal endophyte *Epichloë uncinatum* on litter decomposition of the host grass, *Schedonorus pratensis*. *Plant Ecol.* **2017**, *218*, 1107–1115. [CrossRef]
17. Song, M.; Chai, Q.; Li, X.; Yao, X.; Li, C.; Christensen, M.J.; Nan, Z. An asexual *Epichloë* endophyte modifies the nutrient stoichiometry of wild barley (*Hordeum brevisubulatum*) under salt stress. *Plant Soil* **2015**, *387*, 153–165. [CrossRef]
18. Song, M.; Wang, Y.; Wang, H.; Bao, G.; Li, X. Effects of *Epichloë* endophytes on litter decomposition -- depending on different host species. *Plant Soil* **2022**, *471*, 715–728. [CrossRef]
19. Šnajdr, J.; Cajthaml, T.; Valášková, V.; Merhautová, V.; Petránková, M.; Spetz, P.; Leppänen, K.; Baldrian, P. Transformation of *Quercus petraea* litter: Successive changes in litter chemistry are reflected in differential enzyme activity and changes in the microbial community composition. *FEMS Microbiol. Ecol.* **2011**, *75*, 291–303. [CrossRef]
20. Guerreiro, M.A.; Brachmann, A.; Begerow, D.; Peršoh, D. Transient leaf endophytes are the most active fungi in 1-year-old beech leaf litter. *Fungal Divers.* **2018**, *89*, 237–251. [CrossRef]
21. Chen, Z.; Jin, Y.; Yao, X.; Wei, X.K.; Li, X.; Li, C.; White, J.F.; Nan, Z. Gene analysis reveals that leaf litter from *Epichloë* endophyte-infected perennial ryegrass alters diversity and abundance of soil microbes involved in nitrification and denitrification. *Soil Biol. Biochem.* **2021**, *154*, 108123. [CrossRef]
22. Buyer, J.S.; Zuberer, D.A.; Nichols, K.A.; Franzluebbers, A.J. Soil microbial community function, structure, and glomalin in response to tall fescue endophyte infection. *Plant Soil* **2011**, *339*, 401–412. [CrossRef]
23. Suryanarayanan, T.S. Endophyte research: Going beyond isolation and metabolite documentation. *Fungal Ecol.* **2013**, *6*, 561–568. [CrossRef]
24. Szink, I.; Davis, E.L.; Ricks, K.D.; Koide, R.T. New evidence for broad trophic status of leaf endophytic fungi of *Quercus gambelii*. *Fungal Ecol.* **2016**, *22*, 2–9. [CrossRef]
25. Promputtha, I.; McKenzie, E.H.; Tennakoon, D.S.; Lumyong, S.; Hyde, K.D. Succession and natural occurrence of saprobic fungi on leaves of *Magnolia liliifera* in a tropical forest. *Cryptogam. Mycol.* **2017**, *38*, 213–225. [CrossRef]
26. Osono, T. Role of phyllosphere fungi of forest trees in the development of decomposer fungal communities and decomposition processes of leaf litter. *Can. J. Microbiol.* **2006**, *52*, 701–716. [CrossRef]
27. Koide, R.; Osono, T.; Takeda, H. Colonization and lignin decomposition of *Camellia japonica* leaf litter by endophytic fungi. *Mycoscience* **2005**, *46*, 280–286. [CrossRef]
28. Fukasawa, Y.; Osono, T.; Takeda, H. Effects of attack of saprobic fungi on twig litter decomposition by endophytic fungi. *Ecol. Res.* **2009**, *24*, 1067–1073. [CrossRef]
29. Yang, Z.; Jin, Y.; Hou, F.; Bowatte, S. Soil microbial and chemical responses to foliar *Epichloë* fungal infection in *Lolium perenne*, *Hordeum brevisubulatum* and *Achnatherum inebrians*. *Fungal Ecol.* **2021**, *53*, 101091. [CrossRef]
30. He, X.; Han, G.; Lin, Y.; Tian, X.; Xiang, C.; Tian, Q.; Wang, F.; He, Z. Diversity and decomposition potential of endophytes in leaves of a *Cinnamomum Camphora* plantation in China. *Ecol. Res.* **2012**, *27*, 273–284. [CrossRef]
31. Rojas, X.; Guo, J.; Leff, J.W.; McNear, D.H., Jr.; Fierer, N.; McCulley, R.L. Infection with a shoot-specific fungal endophyte (*Epichloë*) alters tall fescue soil microbial communities. *Microb. Ecol.* **2016**, *72*, 197–206. [CrossRef] [PubMed]
32. Jin, Y.; Wei, X.; White, J.F.; Chen, T.; Li, X.; Chen, Z.; Li, C. Soil fungal and bacterial communities are altered by incorporation of leaf litter containing a fungal endophyte. *Eur. J. Soil Sci.* **2022**, *73*, e13240. [CrossRef]
33. Fukami, T.; Dickie, I.A.; Wilkie, J.P.; Paulus, B.C.; Park, D.; Roberts, A.; Buchanan, P.K.; Allen, R.B. Assembly history dictates ecosystem functioning: Evidence from wood decomposer communities. *Ecol. Lett.* **2010**, *13*, 675–684. [CrossRef] [PubMed]
34. Dickie, I.A.; Fukami, T.; Wilkie, J.P.; Allen, R.B.; Buchanan, P.K. Do assembly history effects attenuate from species to ecosystem properties? A field test with wood-inhabiting fungi. *Ecol. Lett.* **2012**, *15*, 133–141. [CrossRef]
35. Agnihotri, S.; Dutt, D.; Tyagi, C.H.; Kumar, A.; Upadhyaya, J.S. Production and biochemical characterization of a novel cellulose-poor alkali-thermo-tolerant xylanase from *Coprinellus disseminatus* SW-1 NTCC 1165. *World J. Microbiol. Biotechnol.* **2010**, *26*, 1349–1359. [CrossRef]

36. Sinsabaugh, R.L.; Antibus, R.K.; Linkins, A.E.; McClaugherty, C.A.; Rayburn, L.; Repert, D.; Weiland, T. Wood decomposition: Nitrogen and phosphorus dynamics in relation to extracellular enzyme activity. *Ecology* **1993**, *74*, 1586–1593. [CrossRef]
37. Li, X.; Wang, J.; Wang, H.; Tang, Y. Isolation, purification, and partial characterization of acid phosphatase from sweet potato leaves. *Food Sci.* **2015**, *36*, 152–157. (In Chinese)
38. Zhang, S.; Cai, X.; Luo, X.; Wang, S.; Guo, A.; Hou, J.; Wu, R. Molecular cloning and characterization of leucine aminopeptidase gene from *Taenia Pisiformis*. *Exp. Parasitol.* **2018**, *186*, 1–9. [CrossRef]
39. Papa, S.; Pellegrino, A.; Fioretto, A. Microbial activity and quality changes during decomposition of *Quercus ilex* leaf litter in three Mediterranean woods. *Appl. Soil Ecol.* **2008**, *40*, 401–410. [CrossRef]
40. Zhao, Z.; Li, H.; Sun, Y.; Shao, K.; Wang, X.; Ma, X.; Hu, A.; Zhang, H.; Fan, J. How habitat heterogeneity shapes bacterial and protistan communities in temperate coastal areas near estuaries. *Environ. Microbiol.* **2022**, *24*, 1775–1789. [CrossRef]
41. Sinsabaugh, R.L.; Shah, J.J.F. Ecoenzymatic stoichiometry and ecological theory. *Annu. Rev. Ecol. Evol. Syst.* **2012**, *43*, 313–343. [CrossRef]
42. Moorhead, D.L.; Sinsabaugh, R.L.; Hill, B.H.; Weintraub, M.N. Vector analysis of ecoenzyme activities reveal constraints on coupled C, N and P dynamics. *Soil Biol. Biochem.* **2016**, *93*, 1–7. [CrossRef]
43. Huang, Y.; Wu, Z.; Zong, Y.; Li, W.; Chen, F.; Wang, G.G.; Li, J.; Fang, X. Mixing with coniferous tree species alleviates rhizosphere soil phosphorus limitation of broad-leaved trees in subtropical plantations. *Soil Biol. Biochem.* **2022**, *175*, 108853. [CrossRef]
44. Abay, P.; Gong, L.; Luo, Y.; Zhu, H.; Ding, Z. Soil extracellular enzyme stoichiometry reveals the nutrient limitations in soil microbial metabolism under different carbon input manipulations. *Sci. Total Environ.* **2024**, *913*, 169793. [CrossRef] [PubMed]
45. Cui, Y.; Zhang, Y.; Duan, C.; Wang, X.; Zhang, X.; Ju, W.; Chen, H.; Yue, S.; Wang, Y.; Li, S.; et al. Ecoenzymatic stoichiometry reveals microbial phosphorus limitation decreases the nitrogen cycling potential of soils in semi-arid agricultural ecosystems. *Soil Tillage Res.* **2020**, *197*, 104463. [CrossRef]
46. Margenot, A.J.; Calderón, F.J.; Bowles, T.M.; Parikh, S.J.; Jackson, L.E. Soil organic matter functional group composition in relation to organic carbon, nitrogen, and phosphorus fractions in organically managed tomato fields. *Soil Sci. Soc. Am. J.* **2015**, *79*, 772–782. [CrossRef]
47. Veum, K.S.; Goyne, K.W.; Kremer, R.J.; Miles, R.J.; Sudduth, K.A. Biological indicators of soil quality and soil organic matter characteristics in an agricultural management continuum. *Biogeochemistry* **2014**, *117*, 81–99. [CrossRef]
48. Oksanen, J.; Blanchet, F.G.; Friendly, M.; Kindt, R.; Legendre, P.; McGlinn, D.; Minchin, P.R.; O'Hara, R.B.; Simpson, G.L.; Solymos, P.; et al. Vegan: Community Ecology Package (Version 2.5-7). 2020. Available online: https://CRAN.R-project.org/package=vegan (accessed on 5 August 2024).
49. Stegen, J.C.; Lin, X.; Fredrickson, J.K.; Chen, X.; Kennedy, D.W.; Murray, C.J.; Rockhold, M.L.; Konopka, A. Quantifying community assembly processes and identifying features that impose them. *ISME J.* **2013**, *7*, 2069–2079. [CrossRef]
50. Xun, W.; Li, W.; Xiong, W.; Ren, Y.; Liu, Y.; Miao, Y.; Xu, Z.; Zhang, N.; Shen, Q.; Zhang, R. Diversity-triggered deterministic bacterial assembly constrains community functions. *Nat. Commun.* **2019**, *10*, 3833. [CrossRef] [PubMed]
51. Zhang, Z.; Deng, Y.; Feng, K.; Cai, W.; Li, S.; Yin, H.; Xu, M.; Ning, D.; Qu, Y. Deterministic assembly and diversity gradient altered the biofilm community performances of bioreactors. *Environ. Sci. Technol.* **2019**, *53*, 1315–1324. [CrossRef]
52. Stegen, J.C.; Lin, X.; Fredrickson, J.K.; Konopka, A.E. Estimating and mapping ecological processes influencing microbial community assembly. *Front. Microbiol.* **2015**, *6*, 370. [CrossRef]
53. Zheng, H.; Yang, T.; Bao, Y.; He, P.; Yang, K.; Mei, X.; Wei, Z.; Xu, Y.; Shen, Q.; Banerjee, S. Network analysis and subsequent culturing reveal keystone taxa involved in microbial litter decomposition dynamics. *Soil Biol. Biochem.* **2021**, *157*, 108230. [CrossRef]
54. Bastian, M.; Heymann, S.; Jacomy, M. Gephi: An open source software for exploring and manipulating networks. In Proceedings of the International AAAI Conference on Web and Social Media, San Jose, CA, USA, 17–29 May 2009. [CrossRef]
55. Guimerà, R.; Amaral, L.A.N. Functional cartography of complex metabolic networks. *Nature* **2005**, *433*, 895–900. [CrossRef] [PubMed]
56. Tang, S.; Ma, Q.; Marsden, K.A.; Chadwick, D.R.; Luo, Y.; Kuzyakov, Y.; Wu, L.; Jones, D.L. Microbial community succession in soil is mainly driven by carbon and nitrogen contents rather than phosphorus and sulphur contents. *Soil Biol. Biochem.* **2023**, *180*, 109019. [CrossRef]
57. Segata, N.; Izard, J.; Waldron, L.; Gevers, D.; Miropolsky, L.; Garrett, W.S.; Huttenhower, C. Metagenomic biomarker discovery and explanation. *Genome Biol.* **2011**, *12*, R60. [CrossRef]
58. Li, C.; Li, H.; Yao, T.; Su, M.; Ran, F.; Han, B.; Li, J.; Lan, X.; Zhang, Y.; Yang, X.; et al. Microbial inoculation influences bacterial community succession and physicochemical characteristics during pig manure composting with corn straw. *Bioresour. Technol.* **2019**, *289*, 121653. [CrossRef]
59. Wang, Y.; Li, T.; Li, C.; Song, F. Differences in microbial community and metabolites in litter layer of plantation and original Korean pine forests in north temperate zone. *Microorganisms* **2020**, *8*, 2023. [CrossRef] [PubMed]
60. Shenhav, L.; Thompson, M.; Joseph, T.A.; Briscoe, L.; Furman, O.; Bogumil, D.; Mizrahi, I.; Pe'er, I.; Halperin, E. FEAST: Fast expectation-maximization for microbial source tracking. *Nat. Methods* **2019**, *16*, 627–632. [CrossRef] [PubMed]

61. Li, S.; Ren, K.; Yan, X.; Tsyganov, A.N.; Mazei, Y.; Smirnov, A.; Mazei, N.; Zhang, Y.; Rensing, C.; Yang, J. Linking biodiversity and ecological function through extensive microeukaryotic movement across different habitats in six urban parks. *iMeta* **2023**, *2*, e103. [CrossRef]
62. Hu, Z.; Delgado-Baquerizo, M.; Fanin, N.; Chen, X.; Zhou, Y.; Du, G.; Hu, F.; Jiang, L.; Hu, S.; Liu, M. Nutrient-induced acidification modulates soil biodiversity-function relationships. *Nat. Commun.* **2024**, *15*, 2858. [CrossRef] [PubMed]
63. Omacini, M.; Chneton, E.J.; Ghersa, C.M.; Otero, P. Do foliar endophytes affect grass litter decomposition? A microcosm approach using *Lolium multiflorum*. *Oikos* **2004**, *104*, 581–590. [CrossRef]
64. Rudgers, J.A.; Caly, K. Endophyte symbiosis with tall fescue: How strong are the impacts on communities and ecosystems? *Fung. Biol. Rev.* **2007**, *21*, 107–124. [CrossRef]
65. Zhou, Y.; Li, X.; Gao, Y.; Ren, A. Plant endophytes and arbuscular mycorrhizal fungi alter the decomposition of *Achnatherum sibiricum* litter. *Appl. Soil Ecol.* **2022**, *180*, 104616. [CrossRef]
66. Sariyildiz, T.; Anderson, J.M. Variation in the chemical composition of green leaves and leaf litters from three deciduous tree species growing on different soil types. *Forest Ecol. Manag.* **2005**, *210*, 303–319. [CrossRef]
67. Zheng, Z.; Mamuti, M.; Liu, H.; Shu, Y.; Hu, S.; Wang, X.; Li, B.; Xu, L. Effects of nutrient additions on litter decomposition regulated by phosphorus-induced changes in litter chemistry in a subtropical forest, China. *Forest Ecol. Manag.* **2017**, *400*, 123–128. [CrossRef]
68. Hu, D.; Wang, M.; Zheng, Y.; Lv, M.; Zhu, G.; Zhong, Q.; Cheng, D. Leaf litter phosphorus regulates the soil meso- and micro-faunal contribution to home-field advantage effects on litter decomposition along elevation gradients. *Catena* **2021**, *207*, 105673. [CrossRef]
69. Tie, L.; Hu, J.; Peñuelas, J.; Sardans, J.; Wei, S.; Liu, X.; Zhou, S.; Huang, C. The amounts and ratio of nitrogen and phosphorus addition drive the rate of litter decomposition in a subtropical forest. *Sci. Total Environ.* **2022**, *833*, 155163. [CrossRef]
70. Bodenhausen, N.; Horton, M.W.; Bergelson, J. Bacterial communities associated with the leaves and the roots of *Arabidopsis thaliana*. *PLoS ONE* **2013**, *8*, e56329. [CrossRef] [PubMed]
71. Hu, H.; Ye, R.; Pang, L.; Jiang, H.; Tian, K.; Gao, Y.; Ji, Y.; Wang, P.; Yang, J.; Zou, X.; et al. Endophytic bacterium *Bacillus cereus* affects host litter decomposition by regulating soil microbial structure and phosphate mineralization. *Appl. Soil Ecol.* **2023**, *192*, 105092. [CrossRef]
72. Richter, A.; Blei, F.; Hu, G.; Schwitalla, J.W.; Lozano-Andrade, C.N.; Xie, J.; Jarmusch, S.A.; Wibowo, M.; Kjeldgaard, B.; Surabhi, S.; et al. Enhanced surface colonisation and competition during bacterial adaptation to a fungus. *Nat. Commun.* **2024**, *15*, 4486. [CrossRef] [PubMed]
73. Wagg, C.; Schlaeppi, K.; Banerjee, S.; Kuramae, E.E.; van der Heijden, M.G.A. Fungal-bacterial diversity and microbiome complexity predict ecosystem functioning. *Nat. Commun.* **2019**, *10*, 4841. [CrossRef]
74. Chase, J.M. Stochastic community assembly causes higher biodiversity in more productive environments. *Science* **2010**, *328*, 1388–1391. [CrossRef] [PubMed]
75. Dini-Andreote, F.; Stegen, J.C.; van Elsas, J.D.; Salles, J.F. Disentangling mechanisms that mediate the balance between stochastic and deterministic processes in microbial succession. *Proc. Natl. Acad. Sci. USA* **2015**, *112*, E1326–E1332. [CrossRef]
76. McEnany, J.; Good, B.H. Predicting the first steps of evolution in randomly assembled communities. *Nat. Commun.* **2024**, *15*, 8495. [CrossRef]
77. Costa, L.A.; Gusmão, L.F.P. Communities of saprobic fungi on leaf litter of *Vismia guianensis* in remnants of the Brazilian Atlantic Forest. *J. For. Res.* **2017**, *28*, 163–172. [CrossRef]
78. Liu, L. Diversity and Molecular Systematics of Aquatic Fungi in the Karst Plateau Wetlands of Guizhou. Doctoral Dissertation, Guizhou University, Guiyang, China, 2020. (In Chinese)
79. Ma, Y.; Veisenhorn, P.; Guo, X.; Wang, D.; Yang, T.; Shi, Y.; Zhang, H.; Chu, H. Effect of long-term fertilization on bacterial communities in wheat endosphere. *Pedosphere* **2021**, *31*, 538–548. [CrossRef]
80. Islam, M.A.; Karim, A.; Mishra, P.; Dubowski, J.J.; Yousuf, A.; Sarmin, S.; Khan, M.M.R. Microbial synergistic interactions enhanced power generation in co-culture driven microbial fuel cell. *Sci. Total Environ.* **2020**, *738*, 140138. [CrossRef]
81. Sarsan, S.; Pandiyan, A.; Rodhe, A.V.; Jagavati, S. Synergistic interactions among microbial communities. In *Microbes in Microbial Communities*; Singh, R.P., Manchanda, G., Bhattacharjee, K., Panosyan, H., Eds.; Springer: Singapore, 2021; pp. 1–37. [CrossRef]
82. Ho, P.Y.; Nguyen, T.H.; Sanchez, J.M.; DeFelice, B.C.; Huang, K.C. Resource competition predicts assembly of gut bacterial communities in vitro. *Nat. Microbiol.* **2024**, *9*, 1036–1048. [CrossRef]
83. Li, J.; Ma, Q.; Jin, M.; Huang, L.; Hui, D.; Sardans, J.; Peñuelas, J.; O'Connor, P.; Zhu, Y.; Yang, X.; et al. From grasslands to genes: Exploring the major microbial drivers of antibiotic-resistance in microhabitats under persistent overgraving. *Microbiome* **2024**, *12*, 245. [CrossRef]